INSTITUTO NACIONAL DE PESQUISA DA AMAZÔNIA – INPA
DIVISÃO DO CURSO DA PÓS-GRADUAÇÃO EM BIOLOGIA DE ÁGUA DOCE E PESCA INTERIOR - DIBAD

Estudo comparativo da toxicidade e dos mecanismos de ação tóxica de nanopartículas de cobre e cobre em duas espécies de peixes da Amazônia: *Apistogramma agassizii* **e** *Paracheirodon axlerodi*

SUSANA BRAZ MOTA

Manaus, Amazonas
Abril, 2017

SUSANA BRAZ MOTA

Estudo comparativo da toxicidade e dos mecanismos de ação tóxica de nanopartículas de cobre e cobre em duas espécies de peixes da Amazônia: *Apistogramma agassizii* e *Paracheirodon axlerodi*

Orientadora: VERA MARIA FONSECA DE ALMEIDA VAL, Dra.

Coorientador: RAFAEL MENDONÇA DUARTE, Dr.

Dissertação apresentada ao Instituto Nacional de Pesquisas da Amazônia como parte dos requisitos necessários para obtenção do título de Mestre em Ciências Biológicas - subárea Biologia de Água Doce e Pesca Interior.

Manaus, Amazonas

Abril, 2017

Mota, Susana Braz

Estudo comparativo da toxicidade e dos mecanismos de ação tóxica de nanopartículas de cobre e cobre em duas espécies de peixes da Amazônia: *Apistogramma agassizii* e *Paracheirodon axlerodi* / Susana Braz Mota. --- Manaus: 2017

Dissertação (mestrado) --- INPA, Manaus, 2017.
Orientadora: Vera Maria Fonseca de Almeida e Val, Dra.
Co-orientador: Rafael Mendonça Duarte, Dr.
Área de concentração: Biologia de Água Doce e Pesca Interior

1. Nanopartículas de CuO 2.Taxa metabólica 3.Respiração mitocondrial 4.Estresse oxidativo 5.Espécies reativas de oxigênio 6.Peixes ornamentais da Amazônia.

Sinopse: Esse estudo teve como objetivo avaliar o efeito de nanopartículas de cobre e do cobre dissolvido sobre a fisiologia, bioquímica e morfologia de duas espécies de peixes ornamentais da Amazônia. Verificou-se diferentes estratégias metabólicas entre essas duas espécies em resposta à exposição ao nCuO e Cu, indicando que distintos mecanismos de ação tóxica dos contaminantes estão associados à diferenças na sensibilidade entre os grupos aqui estudados.

AGRADECIMENTOS

Agradeço primeiramente à minha mãe, Mila Maria Braga Braz, por ser meu exemplo de amor, luta e dedicação, e por todo o incentivo e contínuo apoio à minha formação acadêmica. Também à minha irmã, Ariel Cristina Braz Mota, pelo companheirismo, pelos conselhos, pelos vários fins de semana que teve que ir me levar ao laboratório e pela oportunidade de poder conviver e aprender com tamanha generosidade.

À minha querida orientadora, Vera Val, pelas discussões, ensinamentos, liberdade, confiança e por me acompanhar passo a passo. Muito obrigada por todas as oportunidades que me foram oferecidas, por sempre me incentivar e confiar na minha capacidade. Acima de tudo, obrigada pelo carinho, dedicação, amizade e por sempre me fazer sentir ser sua filha científica.

Ao meu amor, Derek Campos, por estar sempre comigo, por me apoiar e me incentivar sempre a ser melhor. Te agradeço por todos os momentos que passamos juntos nessa trajetória, pelo amor e pelo cuidado.

Ao professor Adalberto Val, pelas oportunidades, discussões científicas e por me incentivar a seguir no caminho da pesquisa.

Gostaria de agradecer imensamente ao Dr. Newton Falcão, que gentilmente cedeu o equipamento sonicador para o nosso laboratório durante praticamente todo o ano de 2016. Sem a sua ajuda o presente trabalho não teria sido possível.

Ao Laboratório de Química Analítica Ambiental, em especial ao Marcos Alexandre Bolson, pela ajuda na determinação dos elementos no ICP e pelo empenho incansável de tentar descobrir "o mistério das nanopartículas".

À toda a equipe do Laboratório Temático de Microscopia Ótica e Eletrônica, em especial ao Lucas Castanhola Dias, pela ajuda com as análises de microscopia, pelas discussões, amizade e por realmente abraçar o meu projeto e me receber tão bem no seu laboratório.

Ao querido Bill (William R. Driedzic), por ter gentilmente nos fornecido os reagentes para as análises mitocondriais. Sem sua ajuda essa dissertação não teria atingido o nível por nós desejado.

Ao amigo Tyson J. Maccormack, pela caracterização das nanopartículas e pelo interesse e empenho na participação desse projeto.

Ao meu coorientador, Rafael Mendonça Duarte, por sempre estar disponível para responder minhas dúvidas e por fazer parte do meu aprendizado na ciência.

À Helen Sadauskas pelos ensinamentos de base no laboratório durante a minha graduação, por ter sido responsável por me fazer descobrir o mundo da pesquisa e ter despertado em mim a emoção em fazer o que gosta.

Aos amigos queridos do mestrado, Marcele Valle, Danilo Castanho, Valesca Chaves, Carla Mendez, Camila Vieira e Ádria Costa, pelas cervejinhas, churras e festinhas que deixaram esse período da vida acadêmica mais leve.

A todos os colegas do laboratório que ajudaram direta ou indiretamente nesse trabalho, por terem feito tudo ficar mais divertido e por me fazer sentir parte da família LEEM, principalmente ao Derek Campos, Yasmin Dantas, Dino (Waldir Caldas), Dona Val e Grazyelle Sebrenski.

À querida Naza (Nazaré Paula) por sempre cuidar tão bem da gente, pelos momentos de descontração e por ser essa profissional tão competente.

Ao pessoal da secretaria do LEEM, Dona Rai, Claudinha e Raquel, pela ajuda logística do trabalho, sempre prontas para atender nossas requisições.

Ao programa de Pós Graduação em Biologia de Água Doce e Pesca Interior do Instituto Nacional de Pesquisas da Amazônia.

À Coordenação de Aperfeiçoamento de Pessoal de Nível Superior (CAPES), pela concessão da bolsa no período do mestrado.

Ao projeto INCT- ADAPTA, fomentado pelo CNPQ e pela Fundação de Amparo à Pesquisa da Amazônia (FAPEAM), pelo recurso para a elaboração deste trabalho.

“O começo de todas as ciências é o espanto de as coisas serem o que são”.

Aristóteles

RESUMO

Nanopartículas de óxido de cobre (nCuO) são amplamente utilizadas como componentes na fabricação de tintas anti-incrustantes para revestimento de barcos, navios e estruturas submersas e, quando liberadas para o ambiente, podem promover toxicidade para organismos aquáticos. O presente trabalho teve como objetivo avaliar os efeitos das nCuO e do cobre dissolvido em duas espécies de peixes da Amazônia: *Apistogramma agassizii* e *Paracheirodon axelrodi*. Primeiramente foi determinada a toxicidade dos compostos às duas espécies (CL_{50}-96h), e então os peixes foram expostos a 50% da CL_{50} nCuO (*A. agassizii* 375 μg L^{-1} e *P. axelrodi* 460 μg L^{-1}) e 50% da CL_{50} Cu (*A. agassizii* 20 μg L^{-1} e *P. axelrodi* 22,9 μg L^{-1}) por 24, 48, 72 e 96 horas. A taxa metabólica (MO_2), respostas osmorregulatórias, capacidade de fosforilação oxidativa e geração de ROS nas mitocôndrias foram avaliadas, além das respostas de defesa antioxidante e danos morfológicos no epitélio branquial das espécies estudadas. Os resultados mostraram um forte aumento do MO_2 e um maior efeito histopatológico na morfologia das brânquias em *P. axelrodi* expostos ao cobre. Embora o consumo oxigênio não tenha sido alterado após a exposição ao cobre em *A. agassizii*, um aumento evidente foi observado após 48h de exposição ao nCuO. Além disso, estes animais apresentaram aumento no extravasamento de prótons da membrana mitocondrial em resposta à exposição à nCuO e Cu, indicando um desbalanço entre a respiração celular e a produção de ATP, diminuindo assim a Taxa de Controle Respiratório (RCR). Curiosamente, esse desacoplamento foi diretamente relacionado com um aumento da produção de ROS. Nossos resultados revelam diferentes estratégias metabólicas entre as duas espécies estudadas em resposta ao nCuO e Cu, indicando que diferentes mecanismos de ação tóxica dos contaminantes estão associados à sensibilidade intrínseca dessas duas espécies.

ABSTRACT

Copper oxide nanoparticles (nCuO) are widely used in boat antifouling paints, and are released into the environment, inducing toxicity to aquatic organisms. The present study aimed to understand the effects of nCuO and dissolved copper on two ornamental Amazon fish species: *Apistogramma agassizii* and *Paracheirodon axelrodi*. Fish were exposed to 50% nCuO LC_{50} (*A. agassizii* 375 µg L^{-1} and *P. axelrodi* 460 µg L^{-1}) and 50% Cu LC_{50} (*A. agassizii* 20 mg L^{-1} and *P. axelrodi* 22.9 µg L^{-1}) for 24, 48, 72 and 96 hours. Metabolic rate (MO_2), gill osmorregulatory processes, gill mitochondria oxidative phosphorylation capacity and ROS generation, oxidative stress defense and morfological damages were evaluated. Our results showed a strong increase in MO_2 and a higher impairment in its gill's morphology in *P. axelrodi* after the copper exposures. Differently, *A. agassizii* presented an increased proton leak (i.e. uncoupling between respiration and ATP production) in response to nCuO and Cu exposure, thus decreasing their Respiratory Control Rate (RCR). Interestingly, this uncoupling was directly related to an increase in ROS levels. Our findings reveal that the metabolic responses of these two species in response to nCuO and Cu, which are probably caused by the differences between species natural histories, indicating that different mechanisms of toxic action of the contaminants are associated to differences in the sensibility of these two species.

SUMÁRIO

LISTA DE TABELAS

LISTA DE FIGURAS

LISTA DE ABREVIAÇÕES E SIGLAS

- ADP	Adenosina difosfato
- ATP	Adenosina trifosfato
- BSA	Albumina bovina (do inglês – Bovine Serum Albumine)
- CA	Anidrase Carbônica (do inglês – carbonic anhydrase)
- CAT	Catalase
- CDNB	1-chloro-2,4-dinitrobenzene
- DNA	Acido desoxirribonucleico
- COX	Citocromo c oxidase
- ENMs	Nanomateriais
- EPA	Environmental Protection Agency
- ETS	Sistema de transporte de elétrons (do inglês – Electron Transport System)
- $FADH_2$	Dinucleótido de flavina e adenina
- GST	Glutationa-S-Transferase
- GTA	Glutaraldeído
- H_2O_2	Peróxido de hidrogênio
- LM	Microscopia de luz (do inglês – Light microscopy)
- LPO	Lipoperoxidação lipídica
- NKA	Na^+,K^+-ATPase
- $\dot{M}O_2$	Taxa metabólica
- MRC	Células ricas em mitocôndria (do inglês – Mitochondria Rich Cells)
- NADH	Dinucleótido de nicotinamida e adenina
- nm	Nanômetro
- NPs	Nanopartículas
- nCuO	Nanopartículas de óxido de cobre
- Oxphos	Fosforilação oxidativa
- RCR	Controle da taxa respiratória (do inglês – Respiratory Control Ratio)
- ROS	Espécies reativas de oxigênio (do inglês – Reactive Oxygen Species)
- SEM	Microscopia eletrônica de varredura (do inglês – Scaning Electron Microscopy)
- SOD	Superóxido dismutase
- U	Unidade de enzima
- UCP	Proteína desacopladora (do inglês – Uncoupling Protein)
- UV	Radiação ultravioleta

INTRODUÇÃO GERAL

A utilização de nanopartículas (NPs) vem crescendo substancialmente, e esses nanomateriais têm sido incorporados em uma série de compostos produzidos em larga escala para fins comerciais, tais como: aditivos em tintas, plásticos, lubrificantes industriais (Midander et al., 2009), revestimentos anti-incrustantes (Isaza et al., 2011), revestimentos metálicos, cosméticos que tenham função de proteção UV (Klaine et al., 2008), aditivos em pesticidas e solventes organoclorados (Petosa et al., 2010), em revestimentos antimicrobianos (Griffitt et al., 2008) e fungicidas (Mueller e Nowack, 2008), podendo ainda ser utilizados em diagnósticos e aplicações médicas, como agente de contraste de imagem biomédica e terapias contra o câncer (Griffitt et al., 2008; Studer et al., 2010).

Segundo Roco (2003), nanopartículas são materiais com pelo menos uma dimensão com tamanho de 1 a 100 nm, definição adotada pela American Society for Testing Materials e pelo Scientific Committee on Emerging and Newly- Identified Health Risks. Dentre as diversas nanopartículas comercializadas, as de óxido de cobre (nCuO) são amplamente utilizadas como componente na fabricação de tintas anti-incrustantes para revestimento de barcos, navios e estruturas submersas (Perreault et al., 2010), sendo reconhecidas como potencial fonte de contaminação para os ecossistemas aquáticos. O uso dessas tintas gera grande vantagem para a economia, uma vez que apresenta diminuição na presença de organismos incrustantes na calha dos barcos, os quais reduzem a velocidade da embarcação e aumentam o consumo de combustível. Segundo Almeida et al. (2007) essas tintas consistem de um filme polimérico feito, principalmente, de monômeros acrílicos e estirênicos, recoberto por nanopartículas de óxidos de cobre. A decomposição destas tintas pode liberar cobre no ambiente sob formas iônicas solúveis ou sob a forma de NPs, sendo que ambas as formas podem ser tóxicas para os organismo aquáticos (Perreault et al., 2010), incluindo os peixes (Saison et al., 2010).

Em geral, a maioria dos efeitos tóxicos decorrentes de NPs é acentuado devido ao pequeno tamanho desses nanomateriais, o que permite diferentes meios de absorção celular, tais como difusão, fagocitose, pinocitose ou endocitose. Uma vez dentro da célula, as nanopartículas podem interagir diretamente com os sistemas biológicos, podendo ser encontradas em diferentes organelas, tais como as mitocôndrias, ou serem estocadas em vesículas (Lynch et al., 2006; Rothen-Rutishauser et al., 2006; Smart et al., 2006). As nanopartículas de óxido de cobre podem

se dissolver (embora lentamente, ao longo de várias horas ou dias), formando íons de cobre a partir da superfície da partícula, liberando esses íons metálicos para o ambiente e apresentando um alto potencial tóxico para os organismos aquáticos.

Nos peixes, as brânquias são reconhecidas como a principal rota de absorção do cobre (Grosell et al., 2002). A exposição aos íons de cobre (Cu^{2+}) promove um elevado efluxo de Na^{+} nos organismos devido a dois principais fatores: primeiramente pelo fato do Cu^{2+} competir ativamente com os canais de Na^{+} no epitélio branquial, e posteriormente, devido a competição dos íons Cu^{2+} com o Ca^{2+} pela ligação nas proteínas que compõem as junções paracelulares, as quais controlam a permeabilidade do epitélio branquial (Grosell et al., 2002; Laurén e McDonald, 1985). No entanto, a toxicidade das nanopartículas pode ocorrer de maneira diferenciada dos metais dissolvidos, uma vez que estes compostos apresentam um sistema de reatividade dependente da quantidade de energia adicionada à dispersão NPs e das propriedades físicas equímicas. Estas propriedades incluem tamanho de partícula, forma e carga superficial, esta última, medida como potencial zeta. Assim, a capacidade de uma partícula de se agregar com outra irá depender destas propriedades, bem como da energia cinética das partículas, da viscosidade da água e de materiais em suspensão no meio, que irá influenciar diretamente no potencial tóxico (Wu et al., 2016).

Considerando o acima exposto, as nCuO podem apresentar toxicidade tanto por suas características de reatividade, quanto pelos efeitos diretos de íons Cu^{2+} a partir de sua superfície. Griffitt e colaboradores (2009), avaliando os efeitos de nanopartículas de cobre e cobre dissolvido sobre *Danio rerio*, observaram que ambas as formas aumentaram os níveis de cobre acumulado no tecido branquial, mantendo níveis semelhantes após 48 h de exposição a ambos os contaminantes, sugerindo que nos animais expostos a nCuO a absorção de Cu^{2+} dissolvido pelo tecido branquial ocorreu a partir da superfície das nanopartículas de cobre.

Nesse contexto, a toxicidade associada tanto as características intrínsecas de reatividade das NPs, quando a liberação de íons de cobre a partir de sua superfície das dessas partículas, pode promover um aumento direto no gasto energético dos peixes. Campbell e colaboradores (2002) verificaram que espécies de *Oncorhynchus mykiss* expostas ao cobre apresentaram aumento do custo metabólico e disfunções na atividade circadiana. Assim, alterações metabólicas associadas à toxicidade do cobre em peixes de água doce podem afetar diretamente o gasto energético relacionado com a manutenção da homeostase dos organismos. A taxa metabólica basal refere-se à quantidade de energia necessária para a manutenção das funções fisiológicas básicas de um

organismo (Steffensen, 1989). Dessa forma, diversos autores têm evidenciado que a exposição ao cobre resulta em um profundo efeito sobre o metabolismo dos peixes, aumentando as necessidades energéticas e afetando negativamente a quantidade de energia disponível para outras funções biológicas, tais como a reprodução e o crescimento (De Boeck et al., 1997; De Boeck et al., 1995).

Embora a taxa metabólica forneça um bom indicativo da demanda energética, a produção de energia (ATP) ocorre em nível celular nas mitocôndrias. Diversos trabalhos apontam distintas disfunções mitocondriais após a exposição à nanopartículas, levando a alterações nos suprimentos energéticos (Guo et al., 2013; Xiong et al., 2013). Contudo, tanto quanto pode alcançar nosso conhecimento, o presente trabalho é o primeiro avaliando a capacidade de fosforilação oxidativa e produção de ROS nas mitocondrias das brânquias de peixes expostos a nanopartículas de óxido de cobre. Estudos avaliando a respiração celular de animais expostos a NPs de zinco mostraram que essas partículas induziram oxidação lipídica na membrana mitocondrial, o que reduziu drasticamente seu potencial de membrana elétrico, levando à disfunções no funcionamento mitocondrial e a ocorrência de apoptose, uma vez que a mitocôndria é capaz de estocar NPs (Guo et al., 2013). A mitocôndria tem seu potencial de membrana medido, frequentemente, por meio do Sistema de Transporte de Elétrons (ETS), o qual utiliza energia de intermediários altamente energéticos (tais como o NADH e $FADH_2$) para converter prótons livres em energia, por meio da fosforilação do ADP. Dependendo do requerimento energético celular, esse sistema pode ser reduzido ou intensificado, como é o caso da exposição a contaminantes ambientais, como o cobre e as nanopartículas de cobre, influenciando diretamente no suprimento de energia.

Dessa forma, a integridade da membrana mitocondrial é essencial para o bom funcionamento da fosforilação oxidativa (Brookes, 2005). Entretanto, um acúmulo de prótons no espaço intermembrana pode ocasionar um desbalanço no equilíbrio ácido-básico da mitocôndria e ativar proteínas desacopladoras (UCPs - Uncoupling Proteins) que irão atuar permitindo a passagem direta de prótons livres para dentro da matriz mitocondrial, promovendo assim a passagem de prótons (íons H^+) desacoplada da produção de ATP, ou seja, derrame de prótons ou, em inglês, Proton Leak. O H^+ Leak nada mais é do que o estravasamento desse íon livre através da membrana mitocondrial. No entanto, o H^+ leak prejudica a produção de energia, pois impede que haja a formação de ATP, pelo desvio dos H^+ que anteriomente iriam passar pela ATPsintase. Adicionalmente, o H^+ leak pode resultar na produção de espécies reativas de oxigênio (ROS), que consistem em moléculas de oxigênio altamente reativas capazes de promover estresse oxidativo

celular, o qual tem como consequência a desnaturação de proteínas, mutação de DNA e peroxidação lipídica (Richter et al., 1988). Assim, para evitar o estresse oxidativo, a célula ativa mecanismos de defesa antioxidantes a fim de neutralizar o ROS, tais como a enzima superóxido dismutase (SOD) que é responsável por catalisar a conversão do ânion superóxido em peróxido de hidrogênio (H_2O_2), ou a catalase (CAT), que é responsável por degradar o peróxido de hidrogênio (H_2O_2) em água e oxigênio molecular (Asada, 1992, Sies, 1999).

Além das alterações bioquímicas que os peixes podem sofrer após a exposição de contaminantes como as nanopartículas, devido às peculiares condições de águas ácidas e pobres em íons em que os peixes amazônicos vivem naturalmente, algumas espécies apresentam diferentes estratégias para manutenção do seu equilíbrio iônico e ácido-base. Em geral, as espécies de peixes da família Characidae apresentam maior capacidade de transporte iônico nas brânquias, contrastando com espécies de peixes da família Cichlidae, as quais possuem baixa capacidade de transporte (Gonzalez et al., 1997, Gonzalez e Preest, 1999, Gonzalez e Wilson, 2001), sugerindo que o gasto energético para a osmoregulação é diferenciado entre espécies de ambas as famílias. Assim, as espécies *P. axelrodi* (Characidae) e *Apistogramma agassizii* (Cichlidae), considerados de grande importância para o mercado comercial de peixes ornamentais da região amazônica, foram utilizadas como modelos para avaliar os efeitos tóxicos e os principais mecanismos de ação de nCuO e do cobre dissolvido.

OBJETIVOS

Geral

- Avaliar os efeitos tóxicos e os principais mecanismos de ação de nanopartículas de óxido de cobre (nCuO) e do cobre dissolvido em duas espécies de peixes ornamentais da Amazônia: *Apistogramma agassizii* e *Paracheirodon axelrodi*

Específicos

- Determinar a toxicidade de nanopartículas de óxido de cobre, por meio da CL_{50}- 96h, para as espécies *Apistogramma agassizii* e *Paracheirodon axelrodi*.
- Identificar o impacto osmorregulatório da exposição aguda às nCuO e ao cobre dissolvido sobre *A. agassizii* e *P. axelrodi*;

- Avaliar potenciais alterações na respiração mitocondrial das brânquias e verificar possíveis danos oxidativos em *A. agassizii* e *P. axelrodi* expostos ao cobre e as nCuO;
- Identificar e descrever o efeito do cobre dissolvido e das nCuO sobre a morfologia branquial de *A. agassizii* e *P. axelrodi*.

Hipóteses

$H_{1.1}$: *A. agassizii* e *P. axelrodi* apresentam diferentes respostas metabólicas quando expostos à nCuO devido ao fato de apresentarem diferentes estratégias para a regulação iônica.

$H_{1.2}$: Devido ao tamanho reduzido, nCuO serão mais tóxicas para *A. agassizii* e *P. axelrodi* quando comparadas aos efeitos do cobre dissolvido.

$H_{1.3}$: A toxicidade das nCuO em *A. agassizii* e *P. axelrodi* será intensificada ao longo do tempo devido à capacidade desses nanomateriais liberarem partículas e íons gradualmente no meio ambiente.

*Artigo formatado de acordo com as normas da revista Environmental Science and Technology

Comparative study of toxicity and mechanisms for toxic action of copper and copper nanoparticles in two Amazon fish species: dwarf cichlid (*Apistogramma agassizii*) and cardinal tetra (*Paracheirodon axlerodi*)

Abstract

Copper oxide nanoparticles (nCuO) are widely used in boat antifouling paints, and are released into the environment, inducing toxicity to aquatic organisms. The present study aimed to understand the effects of nCuO and dissolved copper on two ornamental Amazon fish species: *Apistogramma agassizii* and *Paracheirodon axelrodi*. Fish were exposed to 50% nCuO LC_{50} (*A. agassizii* 375 µg L^{-1} and *P. axelrodi* 460 µg L^{-1}) and 50% Cu LC_{50} (*A. agassizii* 20 mg L^{-1} and *P. axelrodi* 22.9 µg L^{-1}) for 24, 48, 72 and 96 hours. Metabolic rate (MO_2), gill osmorregulatory processes, gill mitochondria oxidative phosphorylation capacity, ROS generation, oxidative stress defenses, and morfological damages were evaluated after exposure. Our results revealed a strong increase of MO_2 and a higher impairment in its gill morphology in the copper exposures in *P. axelrodi*. Differently, the mitochondria from *A. agassizii* presented an increased proton leak (i.e., uncoupling between respiration and ATP production) in response to nCuO and Cu exposure, thus decreasing their Respiratory Control Rate (RCR). Interestingly, this uncoupling was directly related to an increase in ROS levels. Our findings reveal different metabolic responses between these two species in response to nCuO and Cu, which are probably caused by the differences between species natural histories, indicating that different mechanisms of toxic action of the contaminants are associated to differences in the sensitivity of these two species.

Key-words: CuO nanoparticles, Metabolic Rate, Mitochondria respiration, Oxidative stress, Reactive Oxygen Species, Ornamental Amazon fishes.

1. Introduction

The progressive and substantial increase in the production and use of nanoparticles (NPs) in various industrial sectors have promoted an increase in the input of NPs into aquatic systems.[1,2] Copper oxide nanoparticle (nCuO), in particular, has biocidal, antibacterial, antiviral and anti-fungal properties, and are commonly used in antimicrobial drugs as well as in industrial applications like conductive films, lubrication, nanofluids, catalysis, and electronic devices, among which, inkjet printing.[3,4,5,6,7] Besides, they are widely used in boat antifouling paints and its release into the environment can induce toxicity to aquatic organisms.

Nanoparticles are substances that have structural components smaller than 100 nanometers (nm) in at least one dimension.[8] These nanomaterials can be found in different forms in the environment: fused, aggregated and agglomerated.[9] The surface properties of metal oxide NPs are determined by their acidity constants and zero point of charge[10], which in turn influences their interaction within aquatic systems. Owing its nano-size the nanoparticle can cross cell membranes through diffusion, endocytosis and phagocytosis, and interact with the biological systems, could be stored inside vesicles, such as mitochondria and various other locations.[11,12]

Even at low levels in the environment, waterborne copper ions (Cu^{2+}) are toxicant to freshwater organisms and widely recognized to induce several histo-morphological alterations in target organs (e.g. gills), promoting impairments manly in gas exchange and in Na^+ and Cl^- homeostasis, but also in nitrogen waste excretion, that may negatively affect fish performance and health.[13] These primary effects of Cu on respiration and ionoregulation has been suggested to imbalance the "osmorespiratory compromise" of fish, i.e. increasing in the energy cost (e.g. measured as oxygen consumption rate; $\dot{M}O_2$) for ionic regulation, to counter-act the increased Na^+ efflux and turnover rates induced by Cu exposure[14,15,13]. In these regards, it has been suggested that the main target-mechanisms for acute Cu toxicity in teleost fish are specie-specific. In rainbow trout (*Oncorhynhcus mykiss*), acute Cu exposure seems to have no or negligible effect on oxygen consumption of fish,[16] but exerts a consistent stimulation of Na^+ diffusive losses and a marked inhibition of Na^+ uptake, which was directly linked to the inhibition of Na^+/K^+-ATPase, V-type H^+-ATPase and carbonic anhydrase (CA) in gills of fish.[17] In contrast, common carp (*Cyprinus carpio*) and gibel carp (*Carassius auratus gibel*) exposed to Cu experienced a decline in $\dot{M}O_2$, suggesting that the disruption of aerobic metabolism might be a key factor for acute toxicity in these fish species.[18,16] Furthermore, in despite of the depletion of whole body Na^+ levels, acute Cu

exposure does not inhibit Na^+ uptake in zebrafish (*Danio rerio*) but markedly reduces Ca^{2+} uptake.[19]

In waterborne Cu exposure, accumulation of this ion in gills and internal organs may have a large impact on cellular metabolism and whole respiration, once Cu is a catalytic cofactor of cytochrome c oxidase (COX) in the mitochondrial electron transport system, and can promote a dysfunction in mitochondrial bioenergetics which can exert deleterious effects on metabolic energy production of fish.[20,21] Additionally, evidences have shown that intracellular Cu accumulation beyond the toxicity threshold levels might lead to enhances in generation of reactive oxygen species (ROS) in mitochondria. These increments in ROS production occurs particularly through the redox reactions cycle between Cu^+ and Cu^{2+},[22] which can affect mitochondria respiration and yield alterations in the electron transport capacity, or even in mitochondria membrane integrity, resulting in a lack of functional integrity of mitochondria.[20,21] To avoid the oxidative stress by excessive ROS generation, cells rely biotransformation process, coordinated by enzymes such Glutathione S-transferases (GST) that acts against oxidative damage and peroxidative products of DNA and lipids, and antioxidant enzymatic defense, such as the superoxide dismutase (SOD), that is responsible for catalyzing the conversion of the superoxide anion into hydrogen peroxide (H_2O_2), and catalase (CAT) that then degrades the H_2O_2 into water and molecular oxygen.[23]

Owing to smaller size, it is believed that nCuO can be more harmful to aquatic organism than Cu exposure, although certain studies have been reported that the toxicity of nCuO to some species are quite lower in comparison to Cu toxicity, as seen in zebrafish (*D. rerio*) [24,25] and rainbow trout (*Oncorhynhcus mykiss*)[26,27]. Indeed, in acute waterborne exposure, Cu ions may be released gradually from nanoparticle surface to water, which has been shown to increase the exposure and accumulation of copper to zebrafish[28,29] and rainbow trout.[26] However, to date, the effects of nCuO in the "osmorespiratory compromise" of freshwater teleost fish remains unclear.

Teleost fish living in ion-poor acidic, like "blackwaters" from Amazon displays remarkable adjustments in their metabolism, [31] ionic regulation,[32,33,34] and nitrogen waste excretion,[35,36] to maintain their internal homeostasis in this challenging environment. For example, while Amazonian characidae species (such as *Paracheirodon axelrodi*, *P. innesi*, and *Hemigrammus* sp) display a specialized acidic-insensitive Na^+ transport mechanism in gills (i.e high affinity (low K_m) and high capacity for Na^+ uptake (J_{max})), while the previously studied cichlid fish species (e.g.

Pterophyllum scalare, *Symphysodon discus* and *Apistogramma agassizii*) have shown an acidic-sensitive Na^+ transport system, with low capacity and affinity for Na^+ uptake, and low gill intrinsic permeability.[37,32,34,35] Additionally, the two fish species *P. axelrodi* and *A. agassizii* are very sensitive to copper exposure (LC_{50}-96h values of 40.1 and 45.9 µg Cu L^{-1} in well water, respectively),[38] which, in the case of *P. axelrodi*, seems to be strongly related to increased Na^+ net losses.[39] Overall, it is expected that these different strategies for ionic regulation among Amazon fish, particularly those with different habitats and life styles, such as the active swimmer *P. axerodi* and the resident sedentary *A. agassizii*, may differ in the energy cost for the maintenance of their osmorespiratory compromise. Nevertheless, details of the main target mechanisms for acute Cu toxicity in these fish species, as well as from the relative toxicity and the mechanisms for nCuO toxicity, remains unclear.

Taking into consideration all of the above mentioned aspects, and being aware of the increasing in metals contamination threats in Amazonian waters,[40,41] associated to the increased risk of nanomaterials toxic effects to aquatic organisms,[2] our main goal is to understand the effects of nCuO in two Amazon fish species (*A. agassizii* and *P. axelrodi*) with different adaptative osmorregulatory mechanisms. To reach this objective we meant to: (i) determine the acute toxicity of nCuO (as lethal concentration at 96 h; LC_{50}-96h) to both species *A. agassizii* and *P. axelrodi*; (ii) investigate the effects of sub-lethal exposures (50% of LC_{50}-96h) to Cu and nCuO on the osmorespiratory compromise, Cu accumulation, and oxidative stress responses in both fish species; (iii) verify the effects of sub-lethal exposure (50% of LC_{50}-96h) to Cu and nCuO on the mitochondrial respiration and ROS production in gills of both fish species; (iv) evaluate the effect of both Cu and nCuO in inducing morpho-histological and histopathological alterations in gills of both fish species; and (v) compare the main toxicity mechanisms of Cu and nCuO, between the cichlidae *A. agassizii* and the characidae *P. axelrodi*.

2. Material and methods

2.1. Nanoparticle and characterization

Copper oxide nanoparticles were purchased from Sigma Aldrich (544868). Hydrodynamic diameter and zeta potential were measurements using Malvern Zetasizer Nano ZS (Malvern Instruments) at 25°C. Zeta potential analysis was determined using a Malvern DTS1070 disposable folded capillary cell. Scanning electron microscopy (SEM) was used to confirm

primary particle size. Concentrated exposure stock solutions of 1 mg mL^{-1} were prepared immediately before use. The nCuO was dispersed by sonication (Sonics Vibra-Cell VCX 500) for 10 min, at 80 % of the maximum capacity of the equipment.

2.2. Animals and rearing

A. agassizii and *P. axelrodi* were purchased from ornamental shop in Manaus (Amazonas, Brazil), and transferred to the laboratory of Ecophysiology and Molecular Evolution at INPA, where they were maintained for at least one month in 450 L indoors fiberglass tanks, supplied with continuous aeration and flow through of well water. Throughout the acclimation period fish were once a day fed ground dry commercial trout pellets and were kept on a 12 h light/12 h dark photoperiod. Feeding was suspended 24 h prior to the experiments. There was no mortality observed during all acclimation period. Experimental and holding procedures followed the CONCEA (National Council of Animal use in Research and Education) animal care guidelines and were previously approved by the INPA's animal care committee (protocol number: 026/2015).

2.3. Determination of nCuO toxicity

The toxicity of nCuO to *A. agassizii* and *P. axelrodi* were evaluated throught determination of the lethal concentration at 96 h of exposure (LC_{50}-96h). For this aim, Groups of ten individuals of each species were transferred from the holding tanks to six 1.5 L glass aquariums and allowed to settle for at least 24 h prior to beginning the tests. Then, specimens of *A. agassizii* (0.89±0.07 g) and *P. axelrodi* (0.67±0.04 g) were exposed for 96 h to six nCuO concentrations (real copper concentrations of 400.32, 600.41, 851.76, 102.52, 120.61 and 150.04 µg L^{-1}), beside the control group. All tests were performed in a semi-static system where 80 % of water volume was replaced every 24 h, and each concentration of nCuO tested in replicate. Water samples were collected every 12 h and stored at -20 °C for subsequent copper analysis. Fish mortality at each concentration of nCuO tested was used to calculate the LC_{50}-96h values.

2.4. Sub-lethal experimental series

After the acclimation period, groups of 21 fish specimens of each species were transferred to individual aerated glass tanks filled with 100 mL of well water, and allowed to recover from handily overnight before beginning the experiments to determine the mechanism of nCuO and Cu^{+2} toxicity. fish were exposed for 24, 48, 72 and 96 h to 50% nCuO LC_{50}-96h (i.e. 375 µg Cu L^{-1} to *A. agassizii* and 460 µg Cu L^{-1} to *P. axelrodi*; determined in this study) and to 50% Cu LC_{50}-96h (20 µg Cu L^{-1} to *A. agassizii* and 22.9 µg Cu L^{-1} to *P. axelrodi*), and the control group in water free of contamination. Values of Cu LC_{50}-96h to both fish species were previously determined[38] in similar well water conditions. The same experimental set-up was conducted over three times to evaluate the sub-lethal effects of sub-lethal levels of both copper and copper oxide nanoparticle on (i) the osmoregulatory compromise, whole body copper accumulation, and whole body oxidative damage and antioxidant responses, (ii) the branchial mitochondrial physiology, and (iii) morpho-histological alterations in gills of fish. The experiments followed a semi-static system where 80% of the water volume was replaced every 24 h.

2.4 .1. Effects of Cu and nCuO on the osmorespiratory compromise, copper accumulation and oxidative damage responses

In this experimental series we determined the routine metabolic rate, the activity of the enzymes Na^+/K^+-ATPase (NKA), v-type H^+-ATPase and carbonic anhydrase (CA) in gills, and the concentration of major ions (Na^+, K^+, Ca^{2+}, Mg^{2+} and Cl^-), the accumulation of copper and the activity of glutathione-S-transferase (GST), catalase (CAT), superoxide dismutase (SOD) and lipid peroxidation (LPO) in whole body of fish exposed to 50% Cu LC_{50}-96h and 50% nCuO LC_{50}-96h.

To each treatment and control group, individuals of both species (n=7) were transferred to 70 mL glass chamber immersed in a water bath tank with aerated water. Routine Metabolic rate was determined by the intermittent flow respirometry.[42] The system consists of a recirculation circuit with three phases: flushing ambient (180 s), wait (120 s), and measurement (300 s), all phases constitute a loop. The glass chamber was connected to one pump that was controlled by an automated computer system DAQ-M (Loligo Systems, Tjele, Denmark) to water recirculation in each loop. After 1 h of recovery handling with constant flush in their chambers (this time was

previously established in preliminary tests), metabolic rate was monitored over a period of 4 h. Metabolic rate was calculated as: $MO_2=\Delta O*Vresp*B^{-1}$, where: ΔO is the rate of change in oxygen concentration (mg O_2 h^{-1}), Vresp is the volume of the respirometer chamber, and B is the mass of the individual (kg). After the respirometry procedure, fish were anesthetized in ice and euthanized by medullar section, and gills were removed surgically. Samples of gills and whole body were immediately frozen in liquid nitrogen and stored at -80 °C freezer to further analysis.

The activity of both Na^+/K^+-ATPase and v-type H^+-ATPase in gills of fish were determined by NADH oxidation by the enzyme reaction coupled to the hydrolysis of ATP.[43] The assay is based on the inhibition of the NKA activity by oubaina (2 mM), and of v-type H+ATPase by N-ethylmaleimide (NEM, 2 mM). Gills were homogenized (1:10 w/v) in a buffer (150 mM sucrose, 50 mM imidazol, 10 mM EDTA, 2.5 mM deoxycholic acid, pH 7.5), and centrifuged at 2000 g for 7 min at 4 °C. The supernatants were added in a reaction mixture (30 mM imidazole, 45 mM NaCl, 15 mM KCl, 3 mM $MgCl_2$* 0.4 mM KCN, 1.0 mM ATP, 0.2 NADH mM, 0.1 mM, frutose-1,6-difosfate, 2 mM PEP, 3 UI mL^{-1} pyruvate kinase and 2 UI mL^{-1} lactate dehydrogenase), containing ouabain, or with NEM or without inhibitors. Changes in the absorbance were read over 10 min at 340 nm. The activity of NKA and v-type H^+-ATPase were calculated by the differences between total activity and activities with ouabain and NEM inhibitors, respectively.

The CA activity was quantified according to the assay described by [44], based on [45]. Gills were homogenized (1:10 w/v) in a phosphate buffer 10 mM, pH 7.4 and centrifuged at 2000 g for 5 min at 4 °C. The supernatants (50 µl) were added in 7.5 mL of reaction buffer (225 mM mannitol, 75 mM sucrose, and 10 mM tris-phosphate, pH 7.4), and 1 ml of cold (2.5 °C) distilled water saturated with CO_2. Immediately after the addition of CO_2-saturated water, the reduction in pH was followed for 20 s, with pH readings every 4 s. Carbonic anhydrase specific activity (CAA) was calculated as: $CAA= [(CR/NCR)^{-1}]$ mg^{-1} total protein in the sample (CR: Catalyzed rate and NCR: Non-catalyzed rate).

In water and whole body samples, major cations (Na^+, K^+, Mg^{2+}, Ca^{2+}) and copper concentrations were determined by plasma atomic emission spectrometry (Thermo Scientific iCAP 7600 ICP-OES), while total chloride was measured by the colorimetric assay described by Zall et al[46]. Aqueous ammonia levels were measured using the colorimetric assay developed by Verdouw et al[47].

Whole body homogenates were prepared in buffer containing 20 mM Tris base, 1 mM EDTA, 1 mM dithiothreitol, 50 mM sucrose, 150 mM KCl, pH 7.6, centrifuged at 15.000g for 20 min at 4 °C, and used to determine the levels of GST, SOD, CAT, and LPO in animals (1:10 w/v for GST and SOD and 1:4 w/v for CAT and LPO). GST activity was determined according to Keen et al[48] protocol using 1-chloro-2,4-dinitrobenzene (CDNB) as the substrate. Changes in absorbance were recorded at 340 nm, and the enzyme activity was calculated as nmol CDNB conjugate $min^{-1}mg^{-1}$protein, using a molar extinction coefficient of 9.6 mM cm^{-1}. Superoxide dismutase (SOD) activity was quantified according to method described by McCord and Fridovich[49], in an assay based on the inhibition of cytochrome c reduction rate by the superoxide radical at 550 nm and 25 °C. The enzyme activity is expressed as U SOD mg^{-1} of protein, where 1 U of SOD corresponds to the quantity of enzyme that promoted the inhibition of 50 % of cytochrome c.

To determine the activity of CAT in sample, the inhibition rate of H_2O_2 decomposition was monitored at 240 nm,[50] and expressed as µmol H_2O_2 min^{-1} mg $protein^{-1}$. The LPO levels were quantified in an assay based on the Fe^{+2} to Fe^{+3} oxidation by hydroperoxides in acid medium, in the presence of ferrous oxidation-xylenol orange, at 560 nm.[51] Total protein in gills and whole body samples were determined spectrophotometrically at 595 nm (SpectraMax M2), according to the colorimetric assay described by Bradford[52], using a bovine serum albumin (BSA) as standard.

2.4.2. Effects of Cu and nCuO on mitochondrial respiration and ROS production

At the end of the second series of sub-lethal exposures, 21 fish (n=7 to each experimental condition) were euthanized by severing the spine; gills were surgically removed and immediately analyzed to obtaining their mitochondria functions. In this series, we measured gills ETS, Leak State, ROS ETS, ROS Leak State and RCR.

After the dissection, fish gills were immersed in 2 mL relaxing buffer BIOPS (2.77 mM CaK_2EGTA, 7.23 mM K_2EGTA, 5.77 mM Na_2ATP, 6.56 mM $MgCl_2 \cdot 6H_2O$, 20 mM taurine, 20 mM imidazole, 0.5 mM dithiothreitol, 50 mM K-MES, 15 mM sodium phosphocreatine and 50 mM sucrose, pH 7.1) using the technique described by Gnaiger et al[53]. The gills were dried, weighed, and immerse in 0.5 mL of buffer MiR05 (0.5 mM EGTA, 3 mM $MgCl_2 \cdot 6H_2O$, 60 mM potassium lactobionate, 20 mM taurine, 10 mM KH_2PO_4, 20 mM Hepes, 160 mM sucrose and

1 g L^{-1} BSA, essentially free fatty acid, pH 7.24 at 20°C), and homogenated handily. The homogenate was diluted in 2.5 mL of Mir05 and oxygen consumption was analyzed in an Oxygraph 2k Orouboros.

ROS emission was measured in parallel with mitochondrial respiration. Superoxide dismutase (SOD; at 22.5 U mL^{-1}) was added to catalyze the reaction of the superoxide produced by mitochondria and Horseradish peroxidase (3 U mL^{-1}) was added to catalyze the reaction of hydrogen peroxide with Ampliflu Red (15 μM) and produce the fluorescent product resorufin (detected using an excitation wavelength of 525 nm and ampliometric filter set (AmR); Oroboros Instruments). The resorufin signal was calibrated with additions of exogenous hydrogen peroxide. Oxygen was added into the gas phase above media prior to closing chambers to supersaturate Gills-MiR05. Complex I (CI) substrates (2 mM malate and 10 mM pyruvate) were added to measure state II respiration through CI in the absence of ADP (denoted 'Leak I'). Excess ADP (2.5 mmM) stimulated oxidative phosphorylation (OXP-I, state III respiration), and glutamate (10 mM) was added to saturate CI. Cytochrome c (10 μM) was added to test outer membrane integrity. Phosphorylating respiration with complexs I and II (CI and CII) substrates (OXP-I, II) was measured by the addition of succinate (10 mM). To uncouple mitochondria (denoted 'ETS'), repeated titrations of carbonyl cyanide p-(trifluoromethoxy) phenyl-hydrazone (FCCP, 0.5 μM) were performed. Then, the activity of CI, II and III complexes were inhibited by the addition of rotenone (0.5 μM), malonate (15 mM) and antimycina (1 μM), respectively. RCR was calculated as ETS/Leak state ratio.

2.4.3. Morpho-histological responses in gills of fish exposed to nCuO and Cu

After each time of exposure to the treatments and the control group, 18 fish were removed from aquariums (n=6 to each experimental condition), anesthetized in ice and euthanized by severing the spine. The gills were carefully removed from each fish and immediately immerse in glutaraldehyde (GTA) 2.5% to further evaluation for the presence of histopathology in gills of animals following exposure to 50% Cu LC_{50}-96h and 50% nCuO LC_{50}-96h.

For each fish, gills arches were fixed in 2.5 % GTA for 24 h and dehydrated in ethanol (70 %, 80 % and 96 %). Samples were embedded in paraplast Plus (Sigma Aldrich), and serial sections

of 3-µm thickness tissue were prepared on glass slides, which were stained with hematoxylin and eosin, and then contrasted with Periodic acid–Schiff (PAS). Samples were analyzed at 100" magnification in an optical microscope. Results were expressed as a prevalence of histopathological lesions in branchial tissue, and gill lesion index were determined according to Bernet et al[54]. To assess branchial tissue alterations, indexes based on severity of lesions were calculated by: I = 1 PI + 10 PII + 100 PIII where, stages I, II and III correspond to the degree of lesion, classified as: normal function of the organ (I = 0–10), mild to moderate damage (I = 11–20), moderate to severe (I = 21–50), severe (I = 51–100), and irreparable damage (I > 100).

In addition, gills arches were also fixed in 2.5 % GTA and washed for 24 h with 16 % glycerol for scanning electron microscopy (SEM) analyses. Then, samples were dehydrated in stepwise ethanol solutions in water (30, 50, 70, 90, 95 %) for 20 min at each step, followed by 2 × 20 min rinses in 100 % ethanol. They were then critical point dried in liquid CO_2 (Bal-Tec CPD 030), mounted on aluminum specimen supports and sputter-coated with gold layer in a metalizer (Bal-Ted SCD 050) and examined under a SEM. Samples were imaged with a scanning electron microscopy (LEO 435VP). All the SEM procedure was performed in the Electronic Microscopy Labortory facility from National Institute of Research of the Amazon (INPA), Manaus, Brazil.

2.5. Data analysis

The data are presented as mean±SEM (n= 7 in series 1 and 2; n= 6 in series 3). Prior to the comparative statistical tests, data distribution and homogeneity were checked. Two-way ANOVA was used to determine differences in all analyzed parameters between fish exposed to the treatments (Control, 50% LC_{50} copper and 50% LC_{50} nCuO), and to evaluate the effect of time exposure to the treatments on the parameters (24, 48, 72 and 96h), followed by Tukey post-hoc tests. A significance level of 0.05 was considered in all test procedures. Principal Components Analysis (PCA) was used to determine the relations between dependent variables in each treatment. Histopathological alterations were evaluated semi-quantitatively using the method described by Poleksic and Mitrovic-Tutundzic[55].

3. Results

3.1 Nanoparticle characterization

The characterization of nCuO by its hydrodynamic diameter, zeta potential and SEM images are shown in Fig. 1. The mean hydrodynamic diameter of nCuO nanoparticles was 185 nm, which suggests a substantial aggregation in samples and the presence of different sizes particles in suspension (i.e. a heterogeneous suspension). The mean zeta potential was -18.2 mV, indicating a slightly stable colloid, which fits with the results of the size measurements that showed some aggregation of nanoparticles in water.

3.2 Acute toxicity of CuO nanoparticle to A. agassizii and P. axelrodi

The calculated LC_{50}-96h for nCuO to *A. agassizii* (375 µg L^{-1}) were lower (around 0.12 times) than those observed to *P. axelrodi* (460 µg L^{-1}), demonstrating that *A. agassizii* was slightly more sensitive to nCuO compared to *P. axelrodi* (Fig. 2). In comparison to copper toxicity, nCuO was largely less toxic to both *A. agassizii* and *P. axelrodi*, as seen as by the 18.7 times and 20.1 times higher nCuO LC_{50}-96h, respectively, in relation to their Cu LC_{50}-96h values previously determined in similar well water conditions (Fig. 2).

3.3 Effects of Cu and nCuO on the osmorespiratory compromise and copper accumulation

There were no differences in MO_2 between specimens of *A. agassizii* exposed to both 50% Cu LC_{50}-96h and 50% nCuO LC_{50}-96h and the control group throughout all experiment (Fig. 3A). In fish exposed to 50% nCuO LC_{50}-96h, MO_2 was increased on average 2.0 times after 48, 72 and 96 h in comparison with fish exposed to nCuO for 24 h (Fig. 3A). On the other hand, increases of 3.1, 2.0 and 2.6 times in MO_2 were seen in specimens of *P. axelrodi* after 24, 48 and 72 h of exposure to 50% Cu LC_{50}-96h, respectively, in relation to fish at control group (Fig. 2B). In addition, MO_2 of *P. axelrodi* exposed to copper for 72 h was significantly higher (over 1.8 times) than oxygen consumption measured in fish exposed to 50% nCuO LC_{50}-96h at the same time of exposure (Fig. 3B).

There were no significant effects of exposure to either 50% Cu LC_{50}-96h or 50% nCuO LC_{50}-96h on branchial Na^+/K^+-ATPase activity in both *A. agassizii* and *P. axelrodi*, throughout the entire experiment, in comparison with fish at control group (Figs. 4A and 5A). The activity of

v-type H^+-ATPase in gills of *A. agassizii* was significantly inhibited by 8.9 and 3.5 times after 24 and 96 h of exposure to 50% nCuO LC_{50}-96h, than seen in fish at control group (Fig. 4B). The exposure to copper for 96 h increased over 2.0 times the activity of v-type H^+-ATPase in gills of *A. agassizii*, in comparison with fish exposed for 24 h to the same treatment (Fig. 4B). In addition, fish exposed for 96 h to copper also showed a significant higher (4.7 times) activity of v-type H^+-ATPase in relation to *A. agassizii* exposed for 96 h to 50% nCuO LC_{50}-96h (Fig. 4B). On the other hand, there were no significant effects of the exposures to either 50% Cu LC_{50}-96h or 50% nCuO LC_{50}-96h on the activity of v-type H^+-ATPase in gills of *P. axelrodi* (Fig. 5B).

Interestingly, the exposure to 50% nCuO LC_{50}-96h significantly inhibited (on average 5.5 times) the activity of CA in gills of *A. agassizii* throughout all experiment, in comparison with fish at the control group (Fig. 4C). The exposure to 50% Cu LC_{50}-96h also inhibited the activity of CA in gills of *A. agassizii*, in relation to control fish, but only after 24 h exposure to copper (Fig. 4C). In addition, fish exposed to copper for 24 and 48 h showed CA activity in gills significantly reduced (on average 4.6 times), when compared with specimens of *A. agassizii* exposed to the same treatment after 72 and 96 h (Fig. 4C). The activity of CA in gills of *A. agassizii* exposed to 50% nCuO LC_{50}-96h were also significantly reduced by 9.6 times after 72 h and 3.2 times after 96 h, compared with CA activity in fish exposed to 50% Cu LC_{50}-96h (Fig. 4C). Conversely, in gills of *P. axelrodi* CA activity showed no inhibition, except by fish exposed to 50% nCuO LC_{50}-96h for 72 h (Fig. 5C).

In the specimens of *A. agassizii* exposed to 50% nCuO LC_{50}-96h for 24, 48 and 72 h, the levels of copper in whole body were higher (on average 7.8 times) than in the control group (Table 2). The accumulation of copper in whole body of *P. axelrodi*, in relation to control, was 20.3 times after 96 h exposure to 50% Cu LC_{50}-96h, and 15.7 or 18.8 times after exposure to 50% nCuO LC_{50}-96h for 72 or 96 h, respectively (Table 2). The whole body Na^+ levels of *A. agassizii* were significantly increased by 1.2 times after the exposure for 72 h to both 50% Cu LC_{50}-96h and 50% nCuO LC_{50}-96h, while the exposure to copper for 96 h also increased the concentration of Na^+ by 1.15 times in whole body of fish (Table 2). In addition, Na^+ levels in *A. agassizii* exposed for 72 h to 50% nCuO LC_{50}-96h were higher than those seen in fish exposed to the same treatment at 24 h. In contrast, Na^+ levels in whole body of *P. axelrodi* were significantly reduced on average 1.6 times only after 24 and 48 h of exposure to 50% Cu LC_{50}-96h (Table 2). There were no significant

effects of the exposures to either 50% Cu LC_{50}-96h or 50% nCuO LC_{50}-96h on the levels of Cl^- and Ca^{2+} in whole body of both fish species (Table 2).

The levels of K^+ in whole body of *A. agassizii* were increased by 1.4 times only after 72 h of exposure to 50% nCuO LC_{50}-96h, whereas a significant reduction in K^+ levels (on average 1.3 times) was seen in specimens of *P. axelrodi* after 24, 48 and 72 h of exposure to 50% Cu LC_{50}-96h. In these fish exposed to copper over 24 to 72 h, K^+ levels were reduced in relation to animals exposed to 96 h to 50% Cu LC_{50}-96h, and were also significant dropped in comparison with specimens of *P. axelrodi* exposed to 50% nCuO LC_{50}-96h, at the same experimental periods (Table 2). The levels of Mg^{2+} in whole body of both fish species exposed to either 50% Cu LC_{50}-96h or 50% nCuO LC_{50}-96h were not statistically different from those Mg^{2+} levels seen in whole body of fish at control group. However, Mg^{2+} levels were increased in whole body of *P. axelrodi* specimens exposed to copper for 96h in relation to fish exposed to the same treatment over 24 to 72 h (Table 2).

3.4 Antioxidant responses and cellular oxidative damage mediated by Cu and nCuO

The exposure of *A. agassizii* to 50% nCuO LC_{50}-96h significantly stimulate GST activity in whole body of fish on average 1.8 times after 96 h, in comparison with animals exposed to the same treatment over 24 to 72 h. The activity of GST in these fish was also increased by 1.9 times when compared to animals exposed to copper for 96 h (Table 3). Catalase activity in whole body of *A. agassizii* increased 2.3 times in fish exposed to 50% nCuO LC_{50}-96h, in relation to animals exposed to copper (Table 3). There were no significant effects of the exposure to either 50% Cu LC_{50}-96h or 50% nCuO LC_{50}-96h on the activity of both GST and CAT in whole body of *P. axelrodi* (Table 3). The exposure of *A. agassizii* to 50% nCuO LC_{50}-96h significantly induced the activity of SOD in whole body 1.6 times after 96 h exposure, in comparison to both fish at the control group, and animals exposed to copper over 96 h (Table 3). In whole body of *P. axelrodi*, SOD activity was significantly stimulated 1.8 and 1.5 times after 24 and 48 h of exposure to copper, compared to the control group, and on average 1.4 times in relation to fish exposed to 50% nCuO LC_{50}-96h after 24 and 48 h. In addition, the activity of SOD in whole body of *P. axelrodi* specimens exposed for 24 h to copper was on average 1.4 times higher than those seen in fish exposed to the same treatment after 72 and 96 h (Table 3). The levels of LPO in whole body of *A. agassizii* were significantly increased by 3.1, 2.2 and 2.3 times after 48, 72 and 96h exposure to

50% nCuO LC_{50}-96h, respectively. LPO levels were also higher in fish exposed to 50% nCuO LC_{50}-96h for 48 h compared to both fish exposed to the same treatment after 24 and 72h (on average 1.6 times), and to animals exposed to copper for 48 h (2.9 times). In *P. axelrodi*, LPO levels were stimulated over 2.0 times by the exposure for 96 h to 50% nCuO LC_{50}-96h, compared to the control group (Table 3).

3.5 Effects of nCuO and Cu exposure to Mitochondrial physiology

The exposure to 50% nCuO LC_{50}-96h increased the mitochondrial leak respiration in gills of *A. agassizii* by 3.1, 3.9 and 3.2 times after 24, 48 and 96 h, respectively, in relation to fish at control. In fish exposed to copper for 72 and 96 h leak respiration was improved by 2.7 and 4.0 times, when compared to control group. Also, leak respiration increase in *agassizii* exposed for 24, 48 and 96h to 50% Cu LC_{50}-96h was evident (Fig. 6A). In gills of *A. agassizii*, mitochondrial ROS production in leak state was increased by 3.6 times only after exposure for 72 h to 50% nCuO LC_{50}-96h (Fig, 6A). Leak mitochondrial respiration in gills of *P. axelrodi* was stimulated only after exposure for 24 to 50% nCuO LC_{50}-96h, which was statistically different to fish at both control group and exposed to copper for 24 h (on average 1.5 times), and also to animals exposed to 50% nCuO LC_{50}-96h for 72 and 96 h (on average 1.6 times) (Fig. 6B). Mitochondrial ROS production in leak state in gills of *P. axelrodi* was increased only after the exposure to 50% Cu LC_{50}-96h for 72 h, in comparison with fish at the control group (7.3 times) and to animals exposed to 50% nCuO LC_{50}-96h for 72 h (3.6 times) (Fig. 6B).

The exposure to 50% Cu LC_{50}-96h for 72 and 96 h significantly increased the ETS capacity in mitochondria of *A. agassizii* by 1.8 and 2.1 times, respectively, whereas exposure for 96 h to 50% nCuO LC_{50}-96h improved ETS respiration by 2.2 times, both in relation to control group (Fig. 7A). ETS capacity in specimens of *A. agassizii* exposed for 72 and 96 h to 50% Cu LC_{50}-96h was also significantly higher (on average 1.8 times), in comparison with fish exposed to same treatment for 24 and 48 h, whereas the increased ETS respiration in fish exposed for 96 h to 50% nCuO LC_{50}-96h was also statistically different from fish exposed for 24 and 48 h to the same treatment (1.7 times on average) (Fig. 7A). ETS capacity in mitochondria of *P. axelrodi* was 1.8 times increased after 72 h of exposure to 50% nCuO LC_{50}-96h, in relation to control group (Fig. 7B). After 24 and 72 h of exposure, mitochondrial ETS respiration in gills of *P. axelrodi* specimens at 50% nCuO LC_{50}-96h were significantly higher (2.1 and 1.6 times, respectively) than those seen

in fish exposed to copper. In addition, ETS respiration after exposure to 50% nCuO LC_{50}-96h for 24 h were significantly higher in relation to fish exposed to the same treatment for 96 h (Fig. 7B). There were no significant effects of the exposures to either 50% Cu LC_{50}-96h or 50% nCuO LC_{50}-96h on mitochondrial ROS production at ETS respiration in gills of both fish species (Fig. 7). Respiratory coupling ratio (RCR), measured as a ETS/Leak state ratio, was significantly decreased by 2.1 and 2.5 times in gills of *A. agassizii* only after the exposure to 50% nCuO LC_{50}-96h for 24 and 48 h, respectively (Fig. 8). There were no significant effects of the exposures to either 50% Cu LC_{50}-96h or 50% nCuO LC_{50}-96h on RCR in gills of *P. axlerodi* (Fig. 8).

3.6 Morpho-histological alterations induced by Cu and nCuO

The histopathology analyses confirm that the gills of *A. agassizii* displayed several morphological alterations after 96 h exposure to both 50% nCuO LC_{50}-96h and 50% Cu LC_{50}-96h, but only in fish exposed to 50% nCuO LC_{50}-96h the integrity of gill epithelium was moderate to heavy compromised (Table 4). In these fish species, more frequent alterations after exposure to both 50% nCuO LC_{50}-96h and 50% Cu LC_{50}-96h were lamellar epithelium lifting, aneurism and rupture, and lamellar hyperplasia and hypertrophy (Figure 9). Similarly, gill epithelium of *P. axelrodi* displayed several morphological alterations after 96 h exposure to both 50% nCuO LC_{50}-96h and 50% Cu LC_{50}-96h but, in contrast to *A. agassizii*, moderate to heavy damage in gills function were seen only in fish exposed for 96 h to 50% Cu LC_{50}-96h (Table 4). *P. axelrodi* displayed moderate to heavy damage after 96 h exposure to both 50% Cu LC_{50}-96h and normal gill function 50% nCu LC_{50}-96h (Table 4). The main morphological alterations in gill epithelium displayed by *P. axelrodi* after 96 h exposure to both 50% nCuO LC_{50}-96h and 50% Cu LC_{50}-96h were lamellar hyperplasia and hypertrophy, lamellar fusion, mitochondria rich cells proliferation and mucous cells proliferation (Fig. 10).

When we observed the surface of the gills in SEM analysis, the main alteration found in *A. agassizii* was epithelium with loss of microridges. In *A. agassizii*, they may provide some mechanical protection against trauma an aid in holding mucous secretion to the skin, this fish also showed some aneurism and rupture (Fig 11). Instead, *P. axelrodi* showed some projection in the filament that promotes a hypertrophy in this region both Cu and nCuO exposures, otherwise, this fish also presented epithelium with loss of microridges, mainly under copper exposure.

4. Discussion

In the present study we demonstrated that nCuO negatively affected the mitochondria physiology, increased whole body Cu accumulation, impaired the ionoregulatory mechanism in gills, enhanced the production of ROS, and activated antioxidant enzymes (SOD and CAT) responses, which were not able to avoid lipid peroxidation in gills of *A. agassizii*. Interestingly, these effects were increased mainly after 72 hours, indicating that acute toxic effects of nCuO to *A. agassizii* were time-dependent. On the other hand, dissolved copper was quite more harmful to *P. axelrodi*, while nCuO promoted only minor toxic effects on this fish species. After exposure to Cu, *P. axelrodi* exibithed an increased oxygen consumption rate, a reduced whole body Na^+ and K^+ levels, a stimulated ROS production and SOD activation, which were associated to severe damages in the epithelial gill tissue of these animals. Overall, different metabolic strategies were observed between these two species in response to exposure to nCuO and Cu, indicating that different mechanisms of toxic action of contaminants are associated with differences in osmorregulatory strategies between the groups studied here.

4.1. Acute toxicity of nCuO is lower than Cu toxicity to both *A. agassizii* and *P. axelrodi*

While the physiological impacts of nCuO in fish are unclear and dissolution of ionic copper may also contribute to its toxicity, it is important to distinguish the effects of nanoparticles from dissolved metals. In the present work, *A. agassizii* was slightly more sensitive to nCuO compared to *P. axelrodi*. However, in comparison to Cu LC_{50}-96h values previously obtained [38], nCuO were much less toxic to both *A. agassizii* and *P. axelrodi*. The study of Griffitt et al[24] also observed that *D. rerio* was more sensitive to dissolved copper (LC_{50}-48h of 0.25 mg Cu L^{-1}) than to nCuO (LC_{50}-48h of 1.56 mg Cu L^{-1}) and authors explain that much of the mass of copper nanoparticles was aggregated into larger, micronsized particles that sedimented rapidly such that only 40–50% of the mass of added particles was present in suspension between 2 and 48 h after addition to tanks.

It is important to mention that the nCuO toxicity is due to dissolution of the copper or to the particles themselves. According to nCuO SEM images here analyzed, much of the mass of copper nanoparticles was aggregated; this fact may have contributed for the particles to be sedimented and become less available to the gills. The aggregation is likely driven by the low zeta potential of copper particles observed in the characterization. Nevertheless, it is important to

consider that some authors reported the capability of the nanoparticle to release metal ions from its surface over time[56,57], which might contribute to increased acute toxic responses to nCuO in fish at long-term.

4.2. *A. agassizii* and *P. axelrodi* exhibit different osmorespiratory, Cu accumulation and oxidative stress responses to Cu and nCuO

Respiratory alterations are among the main organismal responses to face environmental challenges. Recent studies have pointed out that different Amazon fish species can present different metabolic and ionoregulatory strategies[37, 34, 31]. One common physiological response to metal ion toxicity is alterations in oxygen uptake in fishes exposed to sub lethal Cu concentrations.[58,18] In the present work, both *A. agassizii* and *P. axelrodi* raised the oxygen consumption following the acute exposure to sub-lethal levels of both nCuO and Cu. During exposure to 50% nCuO LC_{50}-96h, *A. agassizii* slighty increased MO_2 after 48, 72 and 96 h, in comparison with fish exposed to nCuO for 24 h, while there were no effects on MO_2 of *P. axelrodi.* Inversely, *P. axelrodi* experienced a wide increase in MO_2 during the first 72 h of exposure to 50% Cu LC_{50}-96h, which was on average 2.6 times higher than MO_2 seen in fish at control group. Instead, the exposure to copper had no effects on MO_2 of *A. agassizii*. Thus, these results evidenced that both Cu and nCuO have a potential to increase oxygen demand in both studied fish species, suggesting that disruption of aerobic metabolism might be a key mechanism for acute toxicity of Cu and nCuO to Amazon fish species.

Although oxygen consumption is a good index of oxygen demand, the animal metabolim constitute of a set of enzymatic transformations that occur during the cellular activity, where its main function is to obtain and use energy in the form of ATP from oxidate materials. The ATP is essential for the efficient operation of many important enzymes involved in ionoregulatory mechanisms of aquatic organisms, supplying the energy to drive the active transport of ions that are mediated by pumps and co-transporters in the osmoregulatory tissues, such the Na^+K^+ATPase and v-type H^+-ATPase[59]. Indeed, the mechanisms for Cu toxicity in freshwater fish has been proposed to include the inhibition of key enzymatic targets involved in Na^+ uptake, as the activity of Na^+/K^+ATPase, v-type H^+-ATPase and Na^+/H^+ exchanger, as well as the carbonic anhydrase (CA)[13,17]. Our findings reveal that both Cu and nCuO are ionoregulatory toxicants to *A. agassizii*, but these effects were seen in a stronger extent in fish exposed to nCuO than Cu, indicating that, even at sub-lethal levels, copper nanopartciles might be more harmful than copper in promote

ionoregulatory disturbances in this fish species. The exposure to copper resulted in minor impairments on the ionoregulatory responses of *A. agassizii*, where it only inhibited the activity of CA after 24 h. However, in fish exposed to Cu, a progressive increment in the activity of both v-type H^+-ATPase and CA was observed after 96 h, and between 72 to 96 h, respectively, where the activity of both enzymes were kept in similar levels than seen in control, suggesting that the fish was able to attenuate the ionoregulatory toxic effects mediated by Cu exposure. On the other hand, in *A. agassizii* gills the exposure to 50% nCuO LC_{50}-96h resulted in a markedly and specific inhibition of v-type H^+-ATPase activity after 24 and 96 h, and inhibition of CA activity throughout all experimental exposure to nCuO. Previous findings have demonstrated that both enzymes are potential targets for the toxic action of Cu[13,17], and the present results are the first evidence that nCuO can have a similar inhibitory action on the activity of both v-type H^+-ATPase and CA in gills of freshwater fish. In these regards, CA is thought to maintain the intracellular gradient of H^+ ions required to drive Na^+ uptake through the apical v-type H^+-ATPase/Na^+ channels [60], and both CA and v-type H^+-ATPase have been involved in Na^+ uptake and acid secretion of the tropical fish species *D. rerio* under acclimation to acidic conditions[61]. Thus, the fact that both enzymes were simultaneous inhibited by nCuO (at 24 and 96 h of exposure) suggests that the mechanisms for Na^+ uptake in gills of *A. agassizii* involves a coupled mechanism among CA and v-type H^+-ATPase, which also seems to be the main target for the ionoregulatory toxic action of nCuO in these fish species.

Notably, *P. axelrodi* was extremely tolerant to the exposure to sub-lethal levels of both Cu and nCuO, displaying only a slight inhibition of CA in gills after 48 h of exposure to nCuO. Recently, a pharmacological study conducted with different Characidae fish species from Rio Negro have suggested that Na^+ uptake in *P. axelrodi* depends on both the ammonia excretion rates and the supply of H^+ mediated by CA activity[35]. However, although the exposure of *P. axlerodi* to similar levels of dissolved copper used in this study (around 50 µg L^{-1}) resulted in stimulation of Na^+, Cl^- and K^+ losses[39], the exact mechanisms for acute toxicity of copper to this fish species remains unclear. Despite this, it has been proposed that the specialization of high branchial Na^+ uptake system seen in this fish species[37] is a possible explaination for the high tolerance of fish to imbalances in Na^+ regulation induced by high H^+ or Cu levels[39]. Interestingly, the activity of Na^+/K^+-ATPase was not affected by the exposure to either Cu and nCuO in both fish species studied, though inhibition of these enzymes has been recognized as a primary toxic target of Cu to

several freshwater fish species[62,17]. These results possibly reflect that copper accumulation in branchial tissue was below the threshold for the inhibition of this enzyme, or was not enough to the binding of Cu in thiol groups on cysteine residues that would result in interferences of the phosphorylation and transport activity of Na^+/K^+-ATPase in gills of this Amazon fish species.

Copper accumulation was observed in *A. agassizii* only in nCuO exposures, while for *P. axelrodi* this bioaccumulation was evident in both Cu and nCuO exposures. Our results indicate that nanoparticles may dissolve in solution with a consequent release of the metallic ion during the experiments, which contribute to increase bioaccumulation of copper, although it has been observed an aggregation of the particles. Despite in low concentrations, Griffitt et al[24] also observed dissolved copper in the copper nanoparticle treatment, where copper levels were similar following exposure to nanocopper and its soluble fraction. The authors suggested that the mechanisms responsible for the effects of nanocopper are unclear, and probably they do not appear to be mediated only by increased gill uptake. Additionally, *P. axelrodi* accumulated 2-3 times more copper than *A. agassizii*. These differences can be explained by insensitive Na^+ transport system seen in *P. axelrodi*, with very high Na^+ affinities and high Na^+ uptake rates, which appears to be supported through unique and novel mechanisms[37,32,33,35], once Cu^+ may compete by Na^+ for the transport sites, which would increase copper uptake and accumulation by fish.

Some studies have reported that copper particles induce oxidative stress through catalytic production of reactive oxygen species at their surface[63,24]. Oxidative stress and altered physiological responses have been reported as aconsequence of exposure to nanometal[64,56,24]. GST is the first enzyme of the biotransformation phase. In the present work, the activity of this enzyme was substantially increased after exposure to nCuO in *A. agassizii*. Futhermore, SOD, the first enzyme in the line of antioxidant defense, was significantly increased in the whole body of this species and, as consequence, CAT was also increased, demonstrating a higher activity of this enzyme during the convertion of the hydrogen peroxide, which is then degradated into water and molecular oxygen. In general, the activation of this enzymatic system generates oxidative stress, what was also observed throughout the increased LPO values in *A. agassizii*. On the other hand, *P. axelrodi* showed increases in SOD activity in all the times after copper exposure; however, damage in the lipid membranes were only observed after the nCuO exposure for this species, indicating that in the copper exposure, the SOD activity was efficient in neutralize the ROS in the whole body.

4.3. Sub-lethal exposures to Cu and nCuO causes negative effects the mitochondrial respiration and ROS production in gills of both fish species

Capacities of oxidative phosphorylation, proton leak, respiratory coupling ratio and ROS production were altered in different ways in *P. axelrodi* and *A. agassizii* species, indicating a specie-specific metabolic stress in their gills, what could interfere in osmorespiratory compromise of fish. In *A. agassizii*, we observed only increases in the respiratory electron transfer system of mitochondria after 72h exposure to both nCuO and Cu, indicating a higher energy requirement at this time of exposure, thereby increasing ATP production. *A. agassizii* seems to have developed a distinct adjustment of mechanisms to sustain the supply of oxygen to maintain ionoregulatory function of the gills. Once *A. agassizii* has low affinity to Na^+ and in your results, we does not observed a Na^+ efflux, we may affirm that no extra energy was neccesarry to maintain osmoregulatory function. However, Paracheirodon axelrodi that have hight Na^+ affinity increased ETS respiration in order to compensate the Na effux, as showed above. This is the first time that a work showed a relation between oxphos requeriment and ionoreglatory function. In fact, *P. axelrodi* increased both the oxidative phosphorylation (ETS) and oxygen consumption (MO_2), suggesting that an initial supplying of O_2 is in accordance with its metabolic demands.

The integrity of the inner mitochondrial membrane is essential to the function of oxphos, and when this integrity is compromised the H^+ leak occurs[67]. *A. agassizii* increased the leak respiration during all periods analyzed exposure to nCuO and after 72h exposure to Cu^{+2} in this study, indicating a compensation for proton leak, or proton slip, with a consequent lack of availability of H^+ for ATP formation, despite the oxygen consumption continues occurring. Thus, nCuO can cause an acidification of the mitochondria due the accumulation of H^+ in the mitochondrial matrix, disturbing the internal acid-base equilibrium as seen by the alteration in carbonic anhydrase activity.The mitochondria are thought to consume over 90% of the cellular oxygen in unstressed cells and are considered the major sites of aerobic cellular ROS production[66]. In our results, *A. agassizii* showed an increase in the ROS production in ETS after 72h exposed to nCuO, indicating that ROS production in ETS was time-dependent for this species. The subsequent elevation in tissue copper after exposure to nCuO could have resulted in changes in the dissolution of copper into the exposure media from the NPs form over the course of the experiment.

Nevertheless, nCuO was able to uncouple the mitochondria of *P. axelrodi* only in the first 24h. This uncoupling state was promptly avoided and normal RCR was reestablished. Despite that, *P. axelrodi* increased ROS production in ETS, substantially only after copper exposure, and followed the same pattern observed by the increase in metabolic rate of these animals. Furthermore, it was possible to observe that the content of ROS was clearly lower when compared with the *A. agassizii*.

According to Salin et al[65], individuals with higher metabolic rates have lower levels of ROS. In the present work, *P. axelrodi* increased its metabolic rate after copper exposure; this was expected since this species usualy displays basal levels of $\dot{M}O_2$ comparatively higher than the cichlidae species. Moreover, *P. axelrodi* showed comparatively lower ROS levels in relation to *A. agassizii*, even under normal conditions. This seems to be related to these species life-styles, considering that *P. axelrodi* is more active and inhabit streams performing continuous swimming against the flow, and, therefore, presents more suitable mechanisms to deal with oxygen when compared to *A. agassizii*, which is considered a sedentary species that lives in the head streams with low oxygen concentrations. Nonetheless, while some studies related uncoupling process with an increase in ROS generation[68,69], this discution remains to be elucidated. The substantially ROS increase was generated in leak state in all tested times after exposure to nCuO for *A. agassizii*, indicating that oxidation occurred in mitochondria. According to Brand's theory[70] the uncoupling has a key role to survival, where the mitochondrial proton cycle appears be a function very important for the species, where the animal performs uncoupling to survive. Thus, according to this theory, there is a feedback loop between mitochondrial ROS generation and H^+ leak, once H^+ leak can inhibit ROS generation, whereas ROS stimulate H^+ leak. In the present work, *A. agassizii* increased the H^+ leak and ROS levels, dispite maintaining its metabolic rate, indicating an adaptation mechanism of this Cichlidae.

RCR values were lower in *A. agassizii* exposed to nCuO between 24 and 48 h, indicating a higher mitochondria uncoupling capacity in this species. This may reflect an early onset of mitochondrial deterioration, but it also a strategy mechanism for this species, opting for increasing both ETS and Leak state, despite essentially maintaining its metabolic rate. In contrast, better coupling and phosphorylation efficiency were observed in gill mitochondria of *P. axelrodi* exposed

to either Cu and nCuO, showing a better ETS efficiency, whereas the alterations in ETS and leak state were less significant in this fish species.

The maintenance of the integrity of the mitochondria membrane in *P. axelrodi* exposed to nCuO may have contributed for a higher energy production towards ATP synthase, what supplied a subtract for the increase in MO_2, showing that despite this species' better ability to support a higher ionic transport, such mechanisms were impaired by the increase in gill ROS production and compromising of the gills, resulting in an ionic disbalance of Na^+. On the other hand, *A. agassizii* that showed low ionic transport capacity is able to maintain the metabolic rate and uncouple the mitochondrial membrane; what suggests that the mitochondrial useless proton cycle must be offset by some outcome of high benefit to this species.

4.4. Cu and nCuO induces morpho-histological and histopathological alterations in gills of both fish species

Morphological dysfunctions were observed in both the LM and SEM analyses for both species. The main histopathological alterations in the gill tissue of *A. agassizii* were lamellar epithelium lifting and lamellar hyperplasia and hypertrophy, both in LM and SEM. These alterations were more frequent in the treatment with nCuO, showing higher histopathological indexes and effects moderate to heavy damage. According to Bernet et al [54], this gills alterations are associated with regressive and progressive changes in ephytelium; such changes may be a consequence of cellular damage caused by oxidative stress, as observed in gills by ROS production and whole body by antioxidant enzymes of this specie in the present work (Table 2). Additionaly, SEM images revelead some particles in the surface of the gill epithelium only in the treatment with nCuO, which may suggest that these structures are nanoparticles aggregations adhered in the gill epithelium (Figure 11).

In *P. axelrodi*, a massive alteration in the morphological gill structure was observed, indicating a ROS production in the mitochondria of gills, which was able to promote progressive dysfunctions in this epithelium such as hypertrophy and hyperplasia in filament and lamellar epithelium, epithelial lifting, aneurysm, rupture of lamellae epithelium, and proliferation of chloride and mucous cells, that were much more severe in fish exposed to Cu. These results contrast with the studies of Griffitt et al[24], that showed 40% higher proliferation or hypertrophy of

epithelial cells in the interlamellar region of the gill in *D. rerio* after exposure to equivalent concentrations of dissolved copper and nanocopper produced.

As already mentioned by Bernet et al[54] the pattern of histopathologies founded in *P. axelrodi* are associated to regressive and progressive changes in the epithelium. Overal, this fish species showed strutural alterations, what was observed by modifications in tissue as in shape and arrangement of cells, such as observed by the lamellar fusion and lamellar hyperplasia and hypertrophy. Moreover, we observed in fish exposed to Cu, a MRC proliferation, which, although beneficial to ionic regulation, can promote injury to the gas transfer, requiring compensatory mechanisms by the fish to minimize the degree of respiratory impairment associated with the thickening of the diffusion barrier elicited by chloride cell proliferation, and increase oxygen consumption. The strong alterations exibited in gill morfology, sugests that *P. axelrodi* is more sensive to Cu than to nCuO exposure in the same toxicity concentrations. Interestingly, *P. axelrodi* SEM images showed some projections in the gills fillament. Despite this structure being present also in the control, both Cu and nCuO exposure promoted a higher pronouncement of these projections, which may refer to a greater sensitivity of the gill surface of this species.

4.5. Differential toxicity and target mechanisms for acute toxicity of Cu and nCuO between the Cichlid fish *A. agassizii* and the characidae *P. axelrodi*

Herein, both studied species showed different sensibilities to Cu and nCuO exposure. A general idea of the dysfunctions found in each of the species was evidenced in the PCA analyses (Fig. 12), where the species were grouped on opposite sides of the same axis, indicating different physiological functional responses. In general, it seems that *A. agassizii* showed more alterations associated with oxidative stress, which can be observed by the alterations in the antioxidant system (Catalase and SOD activity and LPO levels), besides ETS and Leak state ROS prodution, as these effects seems much more intensified in the nCuO exposures. Instead, *P. axelrodi* showed stronger metabolic effects such as MO_2, Leak State and ETS alterations.

A. agassizii seems to have a mitochondrial adaptation mechanism, once this specie can maintain its metabolic rate, even though uncoupling their mitochondria as a response to the increased ETS. ROS generation process, promote activation of mechanism of oxidant enzymes and the effects in gills lamellar epithelium are reduced. Additionally, all these effects in *A. agassizii* seem to be time-dependent in nCuO exposures, once the effects seem to be intensified after 72 h

of exposure. These results can be supported by the low ionic transport capacity and permeability of gills seen in this fish species, as well as in other species belonging to Cichlidae family, which might directly influence the oxygen consumption, the uptake capacity and metabolization of the compounds. On the other hand, *P. axelrodi* showed more metabolic dysfunctions under exposure to the dissolved copper, and the extent of this impairments was not time-dependent. This Characidae fish specie shows an increase of energetic demands, as observed by the increase in oxygen consumption that can be explained by the intense compromising of the gills morphology. *P. axelrodi* is from Characidae family and present a higher ionic transport capacity in the gills, suggesting that the energy expenditure for osmo and ionoregulation is higher, which may explain the increase in the MO_2 and consequent alterations in the metabolic funtions. Our findings reveal that different mechanisms of toxic action of contaminants are associated with differences in the osmorregulatory strategies among species here studied.

Acknowledgments

The authors thank Marcos Alexandre Bolson for supporting copper analysis and Lucas Castanhola Dias and Laboratório Temático de Microscopia Ótica e Eletrônica for supporting histopathological analysis.

References

(1) Service, R. F. Nanotoxicology. Nanotechnology grows up. *Science*. **2004**, 304, 1732–1734. DOI:10.1126/science.304.5678.1732

(2) Moore, M. N. Do nanoparticles present ecotoxicological risks for the health of the aquatic environment? *Environ. Int.* **2006**, 32, 967–976.

(3) Cheon, J.; Lee, J.; Kim, J. Inkjet printing using copper nanoparticles synthesized by electrolysis. *Thin Solid Films*. **2012**, 520, 2639–2643.

(4) Longano, D.; Ditaranto, N.; Cioffi, N.; Di Niso, F.; Sibillano, T.; Ancona, A.; Conte, A.; Del Nobile, M. A.; Sabbatini, L.; Torsi, L. Analytical characterization of laser-generated copper

nanoparticles for antibacterial composite food packaging. *Anal. Bioanal. Chem.* **2012**, 403, 1179–1186.

(5) De-Jong, W. H.; Borm, P. J. Drug delivery and nanoparticles: Applications and hazards. *Int. J. Nanomedicine*. **2008**, 3, 133-149.

(6) Raffi, M.; Mehrwan, S.; Bhatti, T. M.; Akhter, J. I.; Hameed, A.; Yawar, W.; Hasan, M. Investigations into the antibacterial behavior of copper nanoparticles against *Escherichia coli*. *Ann Microbiol*. **2010**, 60, 75–80. DOI 10.1007/s13213-010-0015-6

(7) Chatterjee, A. K.; Sarkar, R. K.; Chattopadhyay, A. P.; Aich, P.; Chakraborty, R.; Basu, T. A simple robust method for synthesis of metallic copper nanoparticles of high antibacterial potency against *E. coli*. *Nanotechnology*. **2012**, 23, 85–103.

(8) EPA Science Policy Council- Nanotechnology Workgroup. 2007. U.S. U.S. Environmental Protection Agency Nanotechnology White Paper, February, U.S Environmental protectin Agency.

(9) Nowack, B., Bucheli, D.T. Occurrence: behaviour and effects of nanoparticles in the environment. *Environ. Pollut*. **2007**, 150, 5–22.

(10) Hristovski, K.; Baumgardner, A.; Westerhoff, P. Selecting metal oxide nanomaterials for arsenic removal in fixed bed columns: from nanopowders to aggregated nanoparticle media. *J. Hazard. Mater.* **2007**, 147, 265–274.

(11) Lynch, I.; Dawson, K. A. Linse, S. Detecting cryptic epitopes created by nanoparticles. *Sci. STKE*. **2006**, 327, 14.

(12) Smart, S. K.; Cassady, A. I.; Lu, G. Q.; Martin, D. J. The biocompatibility of carbono nanotubes. *Carbon*. **2006**, 44, 1034–1047.

(13) Grosell, M., Copper. In: Farrell, A. P.; Wood, C. M.; Brauner, C. J. (Eds.), Homeostasis and Toxicology of Essential Metals, Fish Physiology. Academic Press, San Diego, **2012**, 31A, 54–110.

(14) Campbell, H. A.; Handy, R. D.; Sims, D. W. Increased metabolic cost of swimming and consequent alterations to circadian activity in rainbow trout (*Oncorhynchus mykiss*) exposed to dietary copper. *Can. J. Fish. Sci.* **2002**, 59, 768-777.

(15) Grosell, M.; Nielsen, C.; Bianchini, A. Sodium turnover rate determines sensitivity to acute copper and silver exposure in freshwater animals. *Comp. Biochem. Physiol. C*. **2002**, 133, 287–303.

(16) De Boeck, G.; van der Ven, K.; Hattink, J.; Blust, R. Swimming performance and energy metabolism of rainbow trout, common carp and gibel carp respond differently to sublethal copper exposure. *Aquat. Toxicol.* **2006**, 80, 92–100.

(17) Chowdhury, M. J.; Girgis, M.; Wood, C. M. Revisiting the mechanisms of copper toxicity to rainbow trout: time course, influence of calcium, unidirectional Na^+ fluxes, and branchial Na^+, K^+ ATPase and V-type H^+ ATPase activities. *Aqua Toxicol.* **2016**, 177, 51–62.

(18) De Boeck, G.; De Smet, H.; Blust, R. The effect of sublethal levels of copper on oxygen consumption and ammonia excretion in the common carp, *Cyprinus carpio*. *Aquat. Toxicol.* **1995**, 32, 127-141.

(19) Alsop, D.; Wood, C. M. Metal uptake and acute toxicity in zebrafish: Common mechanisms across multiple metals. *Aquat. Toxicol.* **2011**, 105, 385–393.

(20) Sappal, R.; MacDonaldb, N.; Fast, M.; Stevens, D.; Kibengea, F.; Siahc, A.; Kamunde, C. Interactions of copper and thermal stress on mitochondrial bioenergetics in rainbow trout, *Oncorhynchus mykiss*. *Aquat. Toxicol.* **2014**, 157, 10–20.

(21) Sappal, R.; MacDougaldc, M.; Fast, M.; Stevens, D.; Kibengea, F.; Siahd, A.; Kamunde C. Alterations in mitochondrial electron transport system activity in response to warm acclimation, hypoxia-reoxygenation and copper in rainbow trout, *Oncorhynchus mykiss*. *Aquat. Toxicol*. **2015**, 165, 51–63.

(22) Linder, M. C.; Hazegh-Azam, M**.** Copper biochemistry and molecular biology. *Am. J. Clin. Nutr*. **1996**, 63, 797-811.

(23) Sies, H. Glutathione and its role in cellular functions. *Free Radical Biol. Med.* **1999**, 27, 916–921.

(24) Griffitt, R. J.; Weil, R.; Hyndman, K. A.; Denslow, N. D.; Powers, K.; Taylor, D.; Barber, D. S. Exposure to copper nanoparticles causes gill injury and acute lethality in zebrafish (*Danio rerio*). *Environ. Sci. Technol.* **2007**, 41, 8178–8186.

(25) Xiong, S.; George, S.; Yu, H.; Damoiseaux, R.; France, B.; Ng, K. W.; Loo, J. S. C. Size influences the cytotoxicity of poly (lactic-co-glycolic acid) (PLGA) and titanium dioxide (TiO_2) nanoparticles. *Arch Toxicol*. **2013**, 87, 1075–1086.

(26) Shaw, B. J.; Al-Bairuty, G.; Handy, R. D. Effects of waterborne copper nanoparticles and copper sulphate on rainbow trout, (*Oncorhynchus mykiss*): Physiology and accumulation. *Aquat. Toxicol*. **2012**, 116–117, 90–101. DOI:10.1016/j.aquatox.2012.02.032

(27) Isani, G.; Falcioni, M. L.; Barucca, G.; Sekar, D.; Andreani, G.; Carpenè E.; Falcioni G. Comparative toxicity of CuO nanoparticles and $CuSO_4$ in rainbow trout. *Ecotoxicol. Environ. Saf*. **2013**, 97, 40–46.

(28) Griffitt, R. J.; Luo, J.; Gao, J.; Bonzongo, J. C.; Barber, D. S. Effects of particle composition and species on toxicity of metallic nanomaterials in aquatic organisms. *Environ. Toxicol. Chem.* **2008**, 27, 1972-1978.

(29) Griffitt, R. J.; Hyndman, K.; Denslow, N. D.; Barber, D. S. Comparison to molecular and histological changes in zebrafish gills exposed to metallic nanoparticles. *Toxicol. Sci*. **2009**, 107, 404–415.

(30) Ivask, A.; Juganson, K.; Bondarenko, O.; Mortimer, M.; Aruoja, V.; Kasemets, K.; Blinova, I.; Heinlaan, M.; Slaveykova, V.; Kahru, A. Mechanisms of toxic action of Ag, ZnO and CuO nanoparticles to selected ecotoxicological test organisms and mammalian cells *in vitro*: A comparative review. *Nanotoxicology*, **2014**, 8, 57–71.

(31) Campos, D. F.; Jesus, T. F.; Kochhann, D.; Heinrichs-Caldas, W.; Coelho, M. M.; Almeida-Val, F.M.F. Metabolic rate and thermal tolerance in two congeneric Amazon fishes: *Paracheirodon axelrodi* Schultz, 1956 and *Paracheirodon simulans* Géry, 1963 (Characidae). *Hydrobiologia*. **2017**, 789, 133–142.

(32) Gonzalez, R. J.; Wilson, R. W.; Wood, C. M.; Patrick, M. L.; Val, A. L. Diverse Strategies for Ion Regulation in Fish Collected from the Ion-Poor, Acidic Rio Negro. *Physiol. Biochem. Zool*. **2002**, 75, 37–47.

(33) Matsuo, A. Y. O.; Val, A. L. Acclimation *to* humic substances *prevents* whole body sodium loss and stimulates branchial calcium uptake capacity *in* cardinal tetras *Paracheirodon axelrodi* (Schultz*)* subjected to extremely low pH. *J. Fish Biol.* **2007**, 70, 989–1000.

(34) Duarte R. M.; Ferreira M. S.; Wood, C. M.; Val, A. L. Effect of low pH exposure on Na^+ regulation in two cichlid fish species of the Amazon. *Comp. Biochem. Physiol. A: Physiol*. **2013**, 166, 441–448.

(35) Wood, C. M.; Robertson, L. M.; Johannsson, O. E.; Val, A. L. Mechanisms of Na^+ uptake, ammonia excretion, and their potential linkage in native Rio Negro tetras (*Paracheirodon axelrodi*, *Hemigrammus rhodostomus*, and *Moenkhausia diktyota*). *J Comp Physiol B*. **2014**, 184, 877–890.

(36) Wood, C. M.; Netto, J. G. S.; Wilson, J. M.; Duarte, R. M.; Val, A. L. Nitrogen metabolism in tambaqui (*Colossoma macropomum*), a neotropical model teleost: hypoxia, temperature, exercise, feeding, fasting, and high environmental ammonia. *J Comp Physiol B*. **2017**, 187, 135–151.

(37) Gonzalez, R. J.; Wilson, R. W. Patterns of ion regulation in acidophilic fish native to the ion-poor, acidic Rio Negro. *J. Fish Biol*. **2001**, 58, 1680–1690.

(38) Duarte, R. M.; Menezes, A. C. L.; Rodrigues, L. S.; Almeida-Val, V. M. F.; Val, A. L. Copper sensitivity of wild ornamental fish of the Amazon. *Ecotoxicol. Environ. Saf*. **2009**, 72, 693–698.

(39) Crémazy, A.; Wood, C. M.; Smith, D. S.; Ferreira, M.S.; Johannsson O. E.; Giacomin, M.; Val, A.L. Investigating copper toxicity in the tropical fish cardinal tetra (*Paracheirodon axelrodi*) in natural Amazonian waters: measurements, modeling, and reality. *Aquat. Toxicol.* **2016**, 180, 353–363.

(40) Silva, M. S. R.; Ramos, J. F.; Pinto, A. G. N. Metais de transição nos sedimentos de Igarapés de Manaus-AM. *Acta Limnol. Bras.* **1999**, 11, 89–100.

(41) Sampaio, A. Q.; 2000. Caracterizac¸ ão física e química dos sedimentos na área do Distrito Industrial de Manaus (AM). Ph.D. Dissertation. Universidade Federal do Amazonas, Manaus, AM Brazil.

(42) Steffensen, J. Some errors in respirometry of aquatic breathers: How to avoid and correct for them. *Fish Physiology* and *Biochemistry*. **1989**, 6, 49-59.

(43) Kültz, D., Somero, G. N. (1995). Osmotic and thermal effects on in situ ATPase activity in permeabilized gill epithelical cells of the fih Gillichthys mirabilis. The Journal of Experimental Biology 198, 1883–1894.

(44) Vitale, A. M.; Monserrat, J. M.; Castilho, P.; Rodriguez, E. M. Inhibitory effects of cadmium on carbonic anhydrase activity and ionic regulation of the estuarine crab *Chasmagnathus granulata* (Decapoda, Grapsidae). *Comp. Biochem. Phys C* . **1999**, 122, 121–129.

(45) Henry, R. P. Techniques for measuring Carbonic Anhydrase activity in vitro. *The Carbonic Anhydrases*. **1991, Chapter 8,** 119-125.

(46) Zall, D. M.; Fisher, D.; Garner, M. Q. Photometric determination of chlorides in water. *Anal. Chem.* **1956**, 28, 1665-1678. Doi: 10.1021/ac60119a009.

(47) Verdouw, H.; Van Echteld, C. J. A.; Dekkers, E. M. J. Ammonia determination based on indophenol formation with sodium salicylate. *Water. Res*. **1978**, 12, 399-402.

(48) Keen, J. H.; Habig, W. H.; Jakobi, W. B. Mechanism for the several activities of the glutathione-S-transferases. *J. Biol. Chem*. **1976**, 251, 6183–6188.

(49) McCord, J.M.; Fridovich, I. Superoxide dismutase, an enzymatic function for erythrocuprein. *J. Biol. Chem.* **1969**, 244, 6049–6055.

(50) Beutler, E. *Red Cell Metabolism: A manual of biochemical methods*. 1975. Grune & Straton, New York.

(51) Jiang, Z. Y.; Woollard, A. C. S.; Wolff, S. P. Lipid hydroperoxide measurement by oxidation of Fe2+ in the presence of xylenol orange. Comparison with the TBA assay and an iodometric method. *Lipids*. **1991**, 26, 853–856. doi:10.1007/BF02536169

(52) Bradford, M. M. A rapid and sensitive method for the quantification of microgram quantities of protein utilizing the protein-dye binding. *Analytical Biochemistry*. **1976**, 72, 248-254.

(53) Gnaiger, E.; Kuznetsov, A. V.; Schneeberger, S.; Seiler, R.; Brandacher, G.; Steurer, W.; Margreiter, R. Mitochondria in the cold. In: Life in the Cold (Heldmaier G, Klingenspor M, eds) Springer, Heidelberg, Berlin, New York: 431-42. 2000.

(54) Bernet, D.; Schmidt, H.; Meier, W.; Burkhardt-Holm, P.; Wahli, T. Histopathology in fish: proposal for a protocol to assess aquatic pollution. *J. Fish. Dis*. **1999**, 22, 25-34.

(55) Poleksic, V., Mitrovic-Tutundzic, V., 1994. Fish gills as a monitor of sublethal and chronic effects of pollution. In: Müller, R., Lloyd, R. (Eds.), Sublethal and Chronic Effects of Pollutants on Freshwater Fish. Cambridge Univ. Press, Cambridge, UK, pp. 339–352.

(56) Siddiqui, S.; Goddard, R. H.; Bielmyer-Fraser, G. K. Comparative effects of dissolved copper and copper oxide nanoparticle exposure to the sea anemone, *Exaiptasia pallida*. *Aquat. Toxicol*. **2015**, 160, 205–213.

(57) Shaw, B. J.; Handy, R. D. Physiological effects of nanoparticles on fish: A comparison of nanometals versus metal ions. *Environ. Int*. **2011**, 37, 1083–1097.

(58) Beaumont, M. W.; Butler, P. J.; Taylor, E. W. Exposure of brown trout to a sublethal concentration of copper in soft acidic water: effects upon gas exchange and ammonia accumulation. *J. Exp. Biol.* **2003**. 206, 153–162.

(59) Marshall, W. S. Na^+, Cl^-, Ca^{2+} and Zn^{2+} transport by fish gills: retrospective review and prospective synthesis. *J. Exp. Zool*. **2002**, 293, 264-283.

(60) Kumai, Y.; Perry, S. F. Mechanisms and regulation of Na^+ uptake by freshwater fish. *Respir Physiol Neurobiol.* **2012**, 184, 249-56.

(61) Yan, J. J.; Chou, M. Y.; Kaneko, T.; Hwang, P. P. Gene expression of Na^+/H^+ exchanger in zebrafish H^+ -ATPase-rich cells during acclimation to low-Na+ and acidic environments. *Am. J. Physiol. Cell Physiol*. **2007**. 293, C1814-C1823.

(62) Láuren, D. J.; McDonald, M. D. Effects of copper on branchial ionoregulation in the rainbow trout, Salmo gairdneri Richardson. *J. Comp. Physiol.* **1985**, 155, 635-644.

(63) Van der Meer, D. L., van den Thillart, G. E., Witte, F., de Bakker, M. A., Besser, J., Richardson, M. K., Spaink, H. P., Leito, J. T. and Bagowski, C. P. (2005). Gene expression profiling of the long-term adaptive response to hypoxia in the gills of adult zebrafish. *Am. J. Physiol*. 289, R1512-R1519.

(64) Callaghan, N. I.; Allen, G. J. P.; Robart, T. E.; Dieni, C. A.; MacCormack, T. J. Zinc oxide nanoparticles trigger cardiorespiratory stress and reduce aerobic scope in the white sucker, *Catostomus commersonii*. *NanoImpact.* **2016**, 2, 29–37.

(65) Salin, K.; Auer, S. K.; Rudolf, A. M.; Anderson, G.; Cairns, A. G.; Mullen, W.; Hartley, R. C.; Selman, C.; Metcalfe, N. B. Individuals with higher metabolic rates have lower levels of reactive oxygen species *in vivo*. *Biol. Lett.* **2015**, 11, 20150538. http://dx.doi.org/10.1098/rsbl.2015.0538

(66) Staniek, K.; Nohl, H. H_2O_2 detection from intact mitochondria as a measure for one-electron reduction of dioxygen requires a non-invasive assay system. *Biochim. Biophys. Acta*. **1999**, 1413, 70–80.

(67) Brookes, P. S. Mitochondrial H^+ leak and ROS generation: An odd couple. *Free Radical Biol. Med*. **2005**, 38, 12– 23.

(68) Turrens, J. F. Superoxide Production by the Mitochondrial Respiratory Chain. *Biosci Rep.* **1997**, 17. DOI: 10.1023/A:1027374931887

(69) Starkov, A. A.; Fiskum, G. Regulation of brain mitochondrial H2O2 production by membrane potencial and NA(P)H redox state. *J. Neurochem*. **2003**, 86, 1101-1107. **DOI:** 10.1046/j.1471-4159.2003.01908.x

(70) Brand, M. D. Uncoupling to survive? The role of mitochondrial inefficiency in ageing. *Exp Gerontol*. **2000**, 35, 811–820

Table 1.

Table 1. Ionic composition, copper and ammnonia concentrations (µM) in water of toxicity tests with *Apistogramma agassizii* and *Paracheirodn axelrodi* after 24, 48, 72 and 96h exposure to 50% of copper LC_{50}-96h, 50% of nanoparticle CuO LC_{50}-96h and control group.

			Na^+	K^+	Ca^{2+}	Mg^{2+}	Cl^-	Cu	NH_4^+
A. agassizii	Control	24h	110.4±1.7	32.5±1.3	0.7±0.09	2.7±0.2	35.6±1.7	2.6±0.1	98.8±26.8
		48h	110.1±3.0	35.6±1.5	0.8±0.1	2.9±0.1	37.1±2.1	2.6±0.09	81.8±19.6
		72h	111.5±3.0	36.3±2.1	0.7±0.06	3.3±0.6	40.6±1.2	2.7±0.07	159.9±22.7
		96h	111.4±0.2	32.6±1.8	0.8±0.18	2.7±0.2	37.6±3.9	2.5±0.1	108.9±7.2
	50% Cu LC_{50}-96h	24h	102.3±2.9	31.4±2.9	1.0±0.1	2.8±0.1	28.8±4.1	18.6±0.2	162.7±26.4
		48h	104.5±2.9	31.7±2.0	1.1±0.1	2.9±0.2	30.7±3.6	18.8±0.1	145.7±20.1
		72h	104.6±5.2	33.5±3.2	0.8±0.1	3.3±0.6	36.3±4.3	18.3±0.3	81.9±15.3
		96h	106.4±4.9	34.8±2.7	1.0±0.1	3.3±0.1	48.2±4.2	18.2±0.1	123.6±11.2
	50% nCuO LC_{50}-96h	24h	105.1±4.5	28.7±2.2	0.7±0.1	3.3±0.3	33.2±5.8	23.0±0.4	122.9±21.5
		48h	107.9±2.3	29.1±3.4	1.2±0.1	3.4±0.3	27.5±5.7	23.5±0.3	82.2±5.1
		72h	102.2±1.2	23.9±1.0	0.9±0.04	3.8±0.6	37.5±4.9	22.8±0.4	134.5±11.2
		96h	104.3±2.3	21.4±0.7	1.0±0.1	3.8±0.9	32.5±6.5	22.9±0.5	131.6±13.2
P. axelrodi	Control	24h	102.6±2.2	25.4±2.2	1.0±0.2	6.3±0.9	28.5±3.4	2.7±0.2	71.3±1.7
		48h	102.1±1.2	23.3±1.2	1.2±0.06	6.1±0.6	32.0±3.5	2.8±0.06	71.8±4.5
		72h	100.5±2.8	26.7±3.1	1.1±0.1	6.0±1.0	31.0±2.7	2.6±0.1	63.5±7.4
		96h	102.5±0.5	25.3±1.5	1.2±0.2	7.1±1.5	30.2±7.3	2.6±0.07	44.1±4.5
	50% Cu LC_{50}-96h	24h	113.1±1.6	32.4±2.7	1.0±0.06	8.4±0.7	50.5±2.2	22.6±0.5	134.8±20.2
		48h	113.4±0.7	31.1±2.8	1.0±0.07	6.0±0.4	47.9±2.0	22.6±0.2	79.5±9.1
		72h	109.6±0.6	34.1±2.6	1.1±0.04	5.6±0.2	42.1±1.0	23.1±0.3	81.3±11.8
		96h	109.0±1.8	27.1±3.0	1.3±0.06	4.8±0.3	40.2±1.4	22.2±0.3	43.7±4.8
	50% LC_{50} nCuO	24h	110.3±0.3	23.6±1.7	0.9±0.1	6.5±0.5	43.8±1.8	28.1±1.5	101.9±8.7
		48h	110.8±1.4	22.6±0.3	0.8±0.07	6.6±0.4	41.6±1.0	29.5±1.1	76.1±5.9
		72h	108.6±0.6	31.5±2.7	1.0±0.03	6.0±0.6	35.8±1.6	28.5±0.6	72.2±7.7
		96h	107.6±1.0	27.1±4.0	1.1±0.06	5.8±0.5	38.4±0.9	30.6±1.4	46.1±4.4

Figure 1.

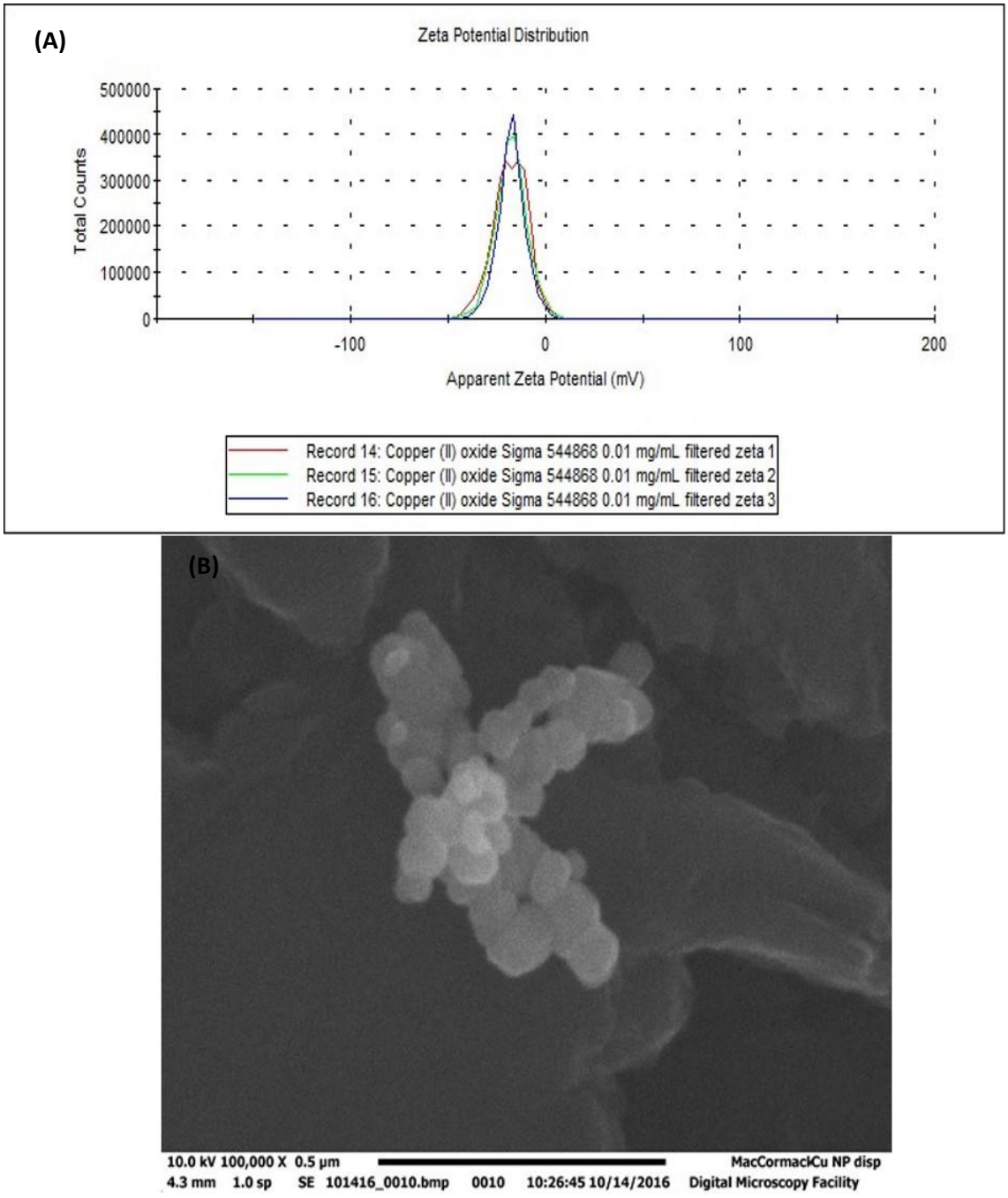

Fig. 1. A) Zeta potential analysis; Data represents average of three replicate measurements on the same sample; B) Scanning electron micrograph of a dried nCuO suspension. Scale bar = 200 nm.

Figure 2.

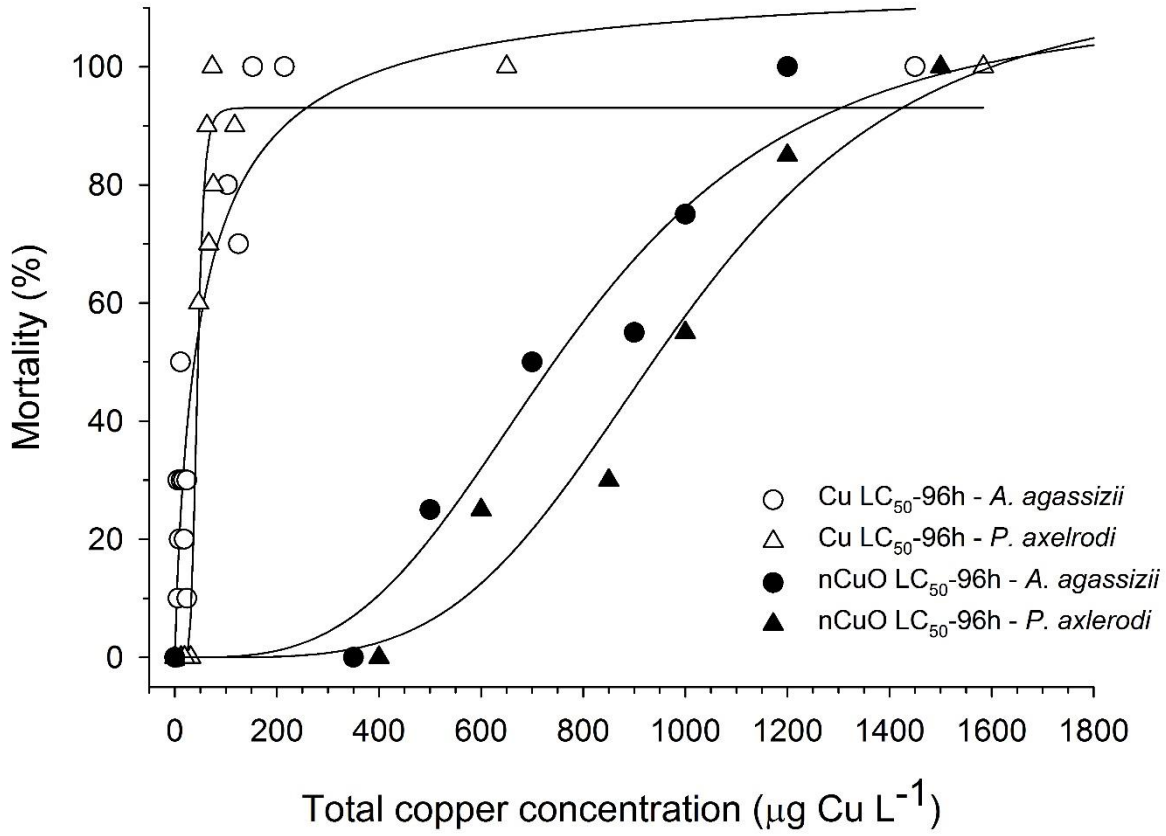

Fig. 2. Relationship between percentage of mortality and real copper concentration in the acute toxicity tests to determine the lethal concentration (LC_{50}-96h) of copper (Cu) and copper oxide nanoparticles (nCuO), to both *Apistogramma agassizii* (circles) and *Paracheirodon axelrodi* (triangles). Black symbols represents the data from the present study with copper oxide nanoparticles, while white symbols represents data of copper toxicity from Duarte et al. (2009).

Figure 3.

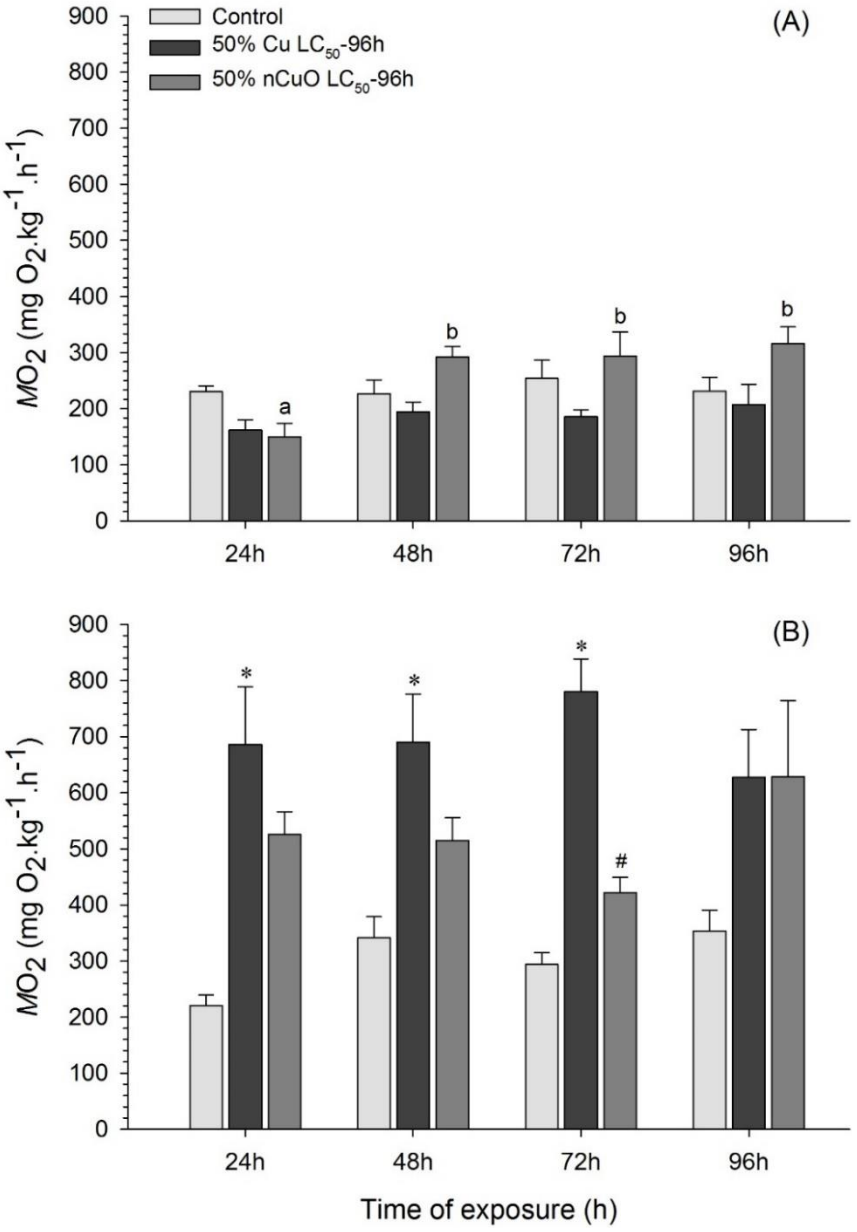

Fig. 3. Oxygen consumption (MO_2) in (A) *Apistogramma agassizii* and (B) *Paracheirodon axelrodi* after 24, 48, 72, and 96 h exposure to either 50% copper LC_{50}-96h and 50% nanparticule CuO LC_{50}-96h, and the control group. Data are presented as Mean±SEM (n=7, at each treatment). Asterisks (*) represent significant differences between the group exposed to either copper or nanoparticle CuO and the control group, at each time of exposure ($p<0.05$). Different letters represent statistical differences between the time of exposure within each treatment ($p<0.05$). Symbol (#) represents significant differences between groups exposed to copper and to nanoparticle CuO at the same time of exposure ($p<0.05$).

Figure 4.

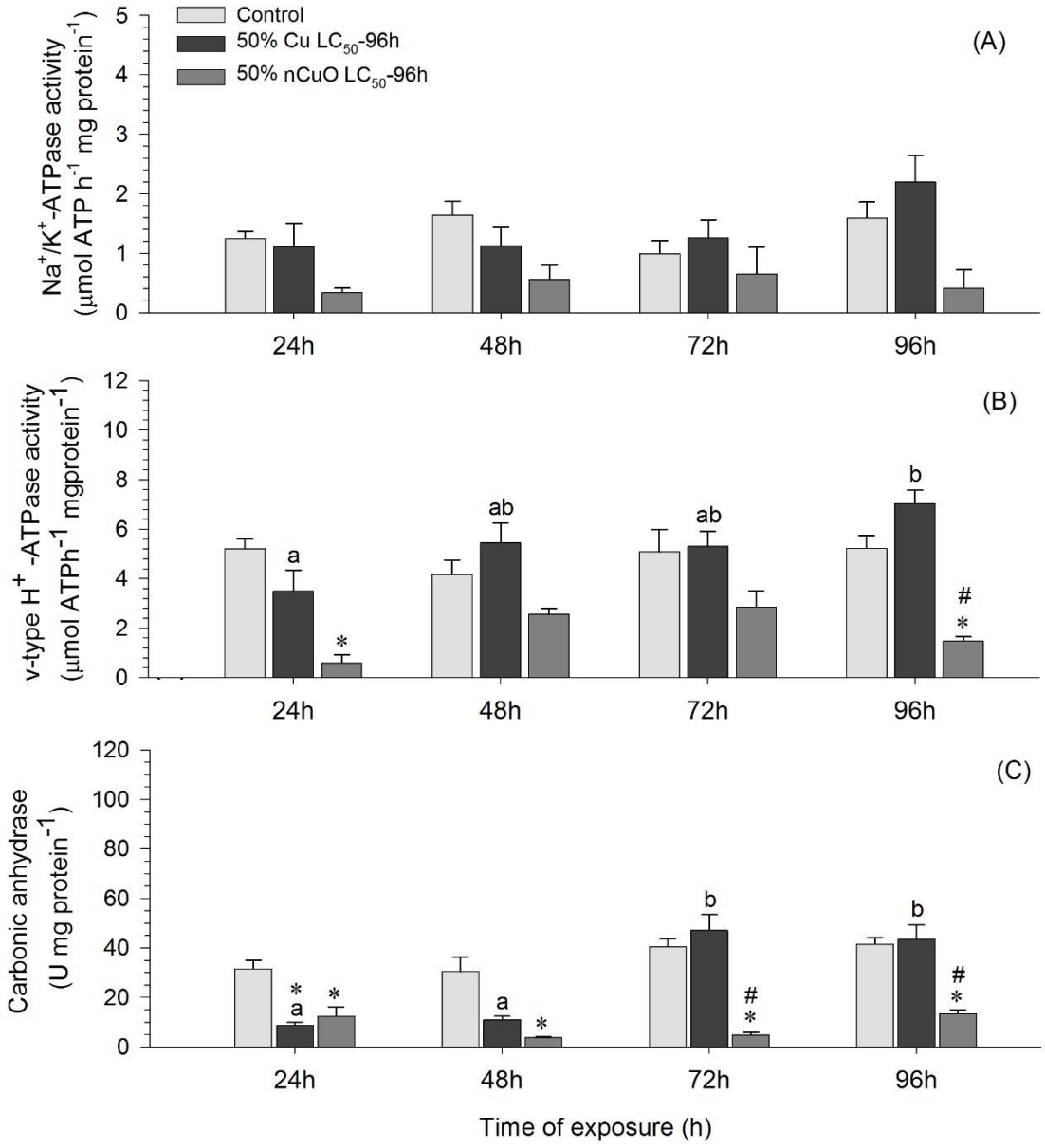

Fig. 4. Branchial activity of Na^+/K^+-ATPase (A), v-type H^+-ATPase (B), and carbonic anhydrase (C) in *Apistogramma agassizii* after 24, 48, 72 and 96 h exposure to either 50% of copper LC_{50}-96h and 50% of nanparticule CuO LC_{50}-96h, and the control group. Data are presented as Mean±SEM (n=7, at each treatment). Asterisks (*) represents significant differences between the group exposed to either copper or nanoparticle CuO and the control group at each time of exposure ($p<0.05$). Different letters represent statistical differences between the time of exposure within each treatment ($p<0.05$). Symbol (#) represents significant differences between group exposed to copper and nanoparticle CuO, at the same time of exposure ($p<0.05$).

Figure 5.

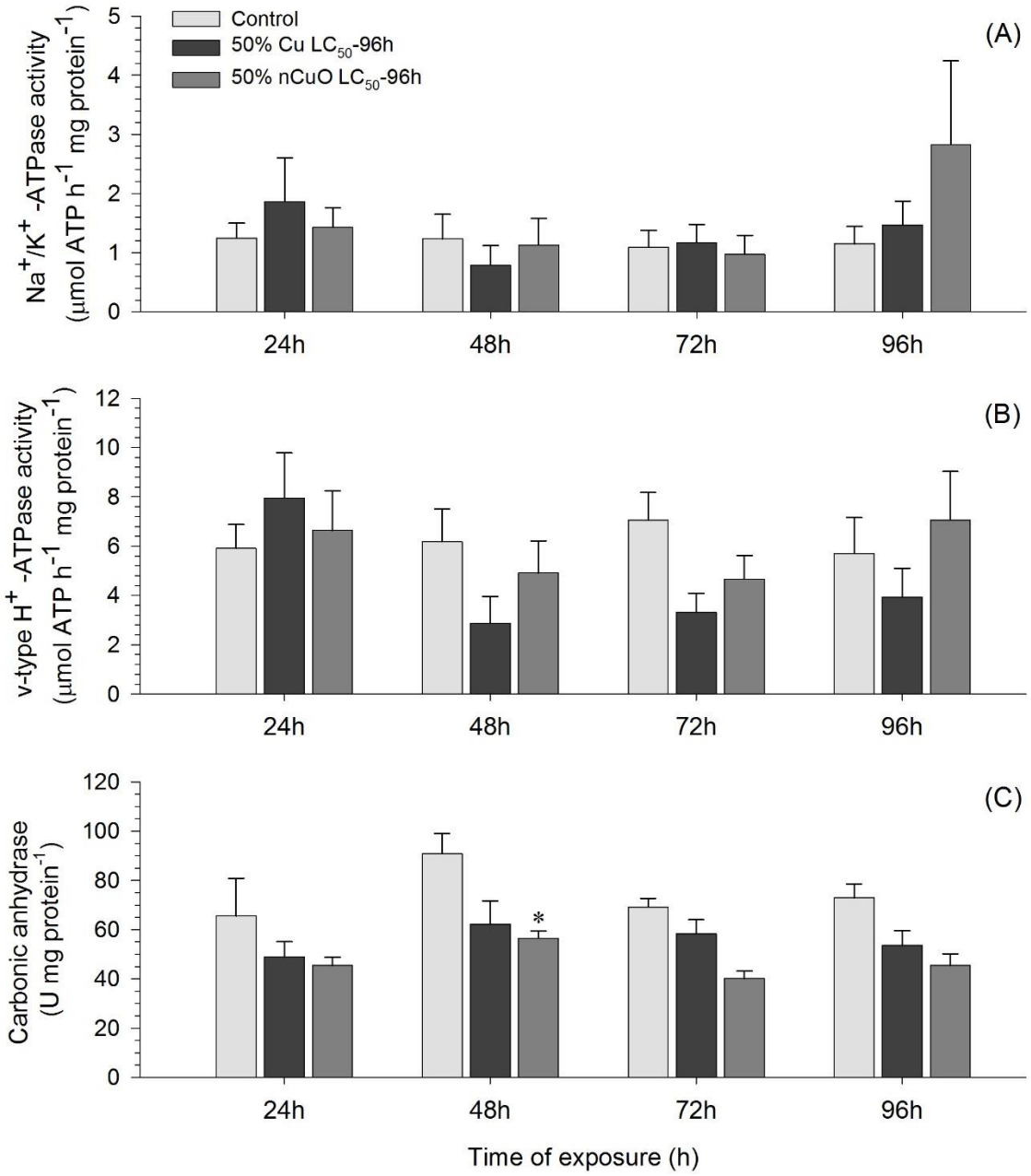

Fig. 5. Branchial activity of Na^+/K^+-ATPase (A), v-type H^+-ATPase (B), and carbonic anhydrase (C) in *Paracheirodon axelrodi* after 24, 48, 72 and 96 h exposure to either 50% of copper LC_{50}-96h and 50% of nanparticule CuO LC_{50}-96h, and the control group. Data are presented as Mean±SEM (n=7, at each treatment). Asterisks (*) represents significant differences between the group exposed to either copper or nanoparticle CuO and the control group at each time of exposure ($p<0.05$). Different letters represent statistical differences between the time of exposure within each treatment ($p<0.05$). Symbol (#) represents significant differences between group exposed to copper and nanoparticle CuO, at the same time of exposure ($p<0.05$).

Table 2. Whole body ionic composition and copper acumulation in *Apistogramma agassizii* and *Paracheirodon axelrodi* exposed to 50% copper LC_{50}-96h, 50% nanoparticule CuO LC_{50}-96h and the control group at diferente times, as indicated.

			Na^+	K^+	Ca^{2+}	Mg^{2+}	Cl^-	Cu
A. agassizii	Control	24h	275.9±4.2	319.4±27.1	140.9±6.8	185.3±6.1	159.3±7.6	0.5±0.1
		48h	272.1±7.0	275.6±18.8	129.3±2.4	179.7±7.4	146.1±2.7	0.6±0.1
		72h	254.5±4.7	272.7±17.5	130.8±4.5	161.0±3.6	147.8±5.1	0.5±0.05
		96h	265.8±9.3	292.6±14.8	127.6±9.4	162.5±12.3	144.2±10.6	0.7±0.1
	50% Cu LC_{50}-96h	24h	296.9±5.3	301.7±13.4	130.7±10.7	226.8±14.8	147.6±12.1	2.4±0.4
		48h	297.6±7.3	328.9±14.0	130.2±18.1	211.7±9.4	147.2±20.4	2.4±0.2
		72h	295.5±3.8*****	317.3±24.7	125.9±9.9	192.0±5.0	142.2±11.2	2.4±0.6
		96h	304.4±5.0*****	282.8±13.2	119.2±4.6	208.7±8.3	134.7±5.2	1.9±0.4
	50% nCuO LC_{50}-96h	24h	275.8±7.2**a**	325.7±12.0	150.1±15.4	253.2±44.0	169.6±17.4	4.1±0.5*****
		48h	290.8±8.0**ab**	314.3±17.1	125.6±5.6	236.3±32.9	141.9±6.4	4.3±1.1*****
		72h	310.3±8.2**b***	380.7±10.1*****	129.9±5.5	223.7±19.7	146.8±6.3	4.1±0.8*****
		96h	285.1±11.7**ab**	365.3±18.7	114.3±2.3	124.4±10.2	129.2±2.6	2.2±0.2
P. axelrodi	Control	24h	100.9±4.3	194.±4.1	70.0±2.6	74.2±1.0	52.2±1.2	0.8±0.2
		48h	99.7±9.8	193.6±2.6	75.3±6.0	73.6±1.8	49.3±2.0	2.0±0.2
		72h	99.0±5.1	182.3±4.7	79.1±3.2	74.8±1.2	56.2±1.8	0.8±0.1
		96h	100.6±4.1	174.9±9.3	72.5±4.5	74.8±1.3	46.0±5.0	0.6±0.1
	50% Cu LC_{50}-96h	24h	60.9±5.4*****	144.6±12.8**a***	75.3±4.8	91.3±4.8**a**	53.7±2.6	8.3±2.3
		48h	63.5±7.6*****	139.9±13.5**a***	96.3±4.9	90.9±7.0**a**	59.5±6.1	9.2±2.9
		72h	81.81±5.0	145.0±8.6**a***	88.0±9.9	91.7±5.1**a**	61.0±3.7	7.0±1.6
		96h	87.89±4.7	192.3±4.5**b**	78.6±17.6	103.5 ±2.0**b**	63.0±9.4	12.2±4.7*****
	50% LC_{50} nCuO	24h	83.71±1.8	188.9±4.4#	68.0±11.2	87.5±9.7	52.5±1.5	5.7±2.0
		48h	86.86±4.6	195.4±7.1#	71.5±7.05	89.0±10.6	52.9 ±3.7	8.8±1.3
		72h	94.90±6.3	195.6±3.2#	68.2±9.8	93.8±5.7	53.6 ±3.5	12.6±1.7*****
		96h	89.98±2.8	183. 6±5.3	69.4±12.4	95.2±8.1	56.7 ±3.4	11.3±1.8*****

Asterisks (*) represents significant differences between the group exposed to either copper or nanoparticle CuO and the control group, at each time of exposure ($p<0.05$).
Different letters represent statistical differences between the time of exposure within each treatment ($p<0.05$).
(#) represents significant differences between group exposed to copper and nanoparticle CuO, at the same time of exposure ($p<0.05$).

Table 3. Activities of enzymes gluthatione-S-transferase (GST) and superoxide dismutase (SOD) (U min^{-1} mg $protein^{-1}$), catalase (CAT) (µM H_2O_2 min^{-1} mg $protein^{-1}$) and lipid peroxidation (LPO) (µM cumene hydroperoxide mg $protein^{-1}$) in whole body of *Apistogramma agassizii* and *Paracheirodon axelrodi*, after 24, 48, 72, and 96 h exposure to either 50% of copper LC_{50}-96 h and 50% of nanoparticle CuO LC_{50}-96 h, and the control group (n=6 at each treatment).

			GST	*SOD*	*CAT*	*LPO*
A. agassizii	Control	24h	242.4± 19.7	18.1± 0.3	173.2± 17.2	30.1± 2.3
		48h	265.1± 16.3	19.0± 0.5	175.1± 20.7	28.7± 1.1
		72h	260.3± 16.2	18.7± 0.4	178.4± 16.0	25.7± 2.8
		96h	218.7± 16.1	19.5± 1.0	181.1± 16.6	26.7± 2.4
	50% Cu LC_{50}-96h	24h	178.9± 20.9	18.6± 1.0	181.2± 12.6	31.7± 2.9
		48h	239.8± 9.8	19.3± 1.1	287.2± 48.2	31.2± 3.2
		72h	252.0± 29.6	19.9± 0.5	254.6± 45.9	40.5± 8.2
		96h	163.1± 25.9	19.4± 0.6	204.9± 38.1	40.9± 6.9
	50% nCuO LC_{50}-96h	24h	191.4± 23.1**a**	23.7± 3.0	322.1± 36.3	53.0± 7.1 **a**
		48h	177.4± 40.2**a**	23.1± 4.3	191.0± 33.0	90.1± 12.4**b*#**
		72h	155.5± 16.3**a**	24.7± 0.6	357.2± 68.5	57.3± 6.2**a***
		96h	315.1± 27.6**b#**	31.7± 3.2***#**	422.9± 109.7*	63.4± 7.6**ab***
P. axelrodi	Control	24h	444.0± 65.5	16.2 ± 0.9	97.5 ± 14.7	27.7± 2.5
		48h	487.2± 34.8	15.3± 1.1	103.1± 15.2	24.9± 3.0
		72h	457.1± 31.5	17.2± 0.6	105.2± 3.8	26.9± 3.0
		96h	332.8± 42.2	15.6± 0.6	68.9± 13.4	22.7± 1.3
	50% Cu LC_{50}-96h	24h	425.9± 41.5	29.2± 2.4**a***	115.1± 21.7	33.2± 4.0
		48h	345.2± 36.2	23.7± 1.1**ab***	130.5± 34.3	31.9± 2.5
		72h	415.8± 45.9	20.3± 0.8**b**	101.7± 14.9	31.8± 2.4
		96h	415.2± 47.0	20.9± 1.2**b**	80.3± 12.8	31.3± 3.9
	50% LC_{50} nCuO	24h	366.6± 19.0	19.8± 1.8#	85.1± 25.1	27.9± 1.4
		48h	349.3± 31.3	17.0± 0.9#	72.3± 17.5	38.7± 10.5
		72h	287.8± 56.7	16.4± 1.3	60.5± 18.7	27.9± 4.5
		96h	377.1± 29.4	21.7± 1.6	61.4± 14.3	47.2± 7.3*

Asterisks (*) represents significant differences between the group exposed to either copper or nanoparticle CuO and the control group at each time of exposure ($p<0.05$).
Different letters represent statistical differences between the time of exposure within each treatment ($p<0.05$).
(#) represents significant differences between group exposed to copper and nanoparticle CuO, at the same time of exposure ($p<0.05$).

Figure 6.

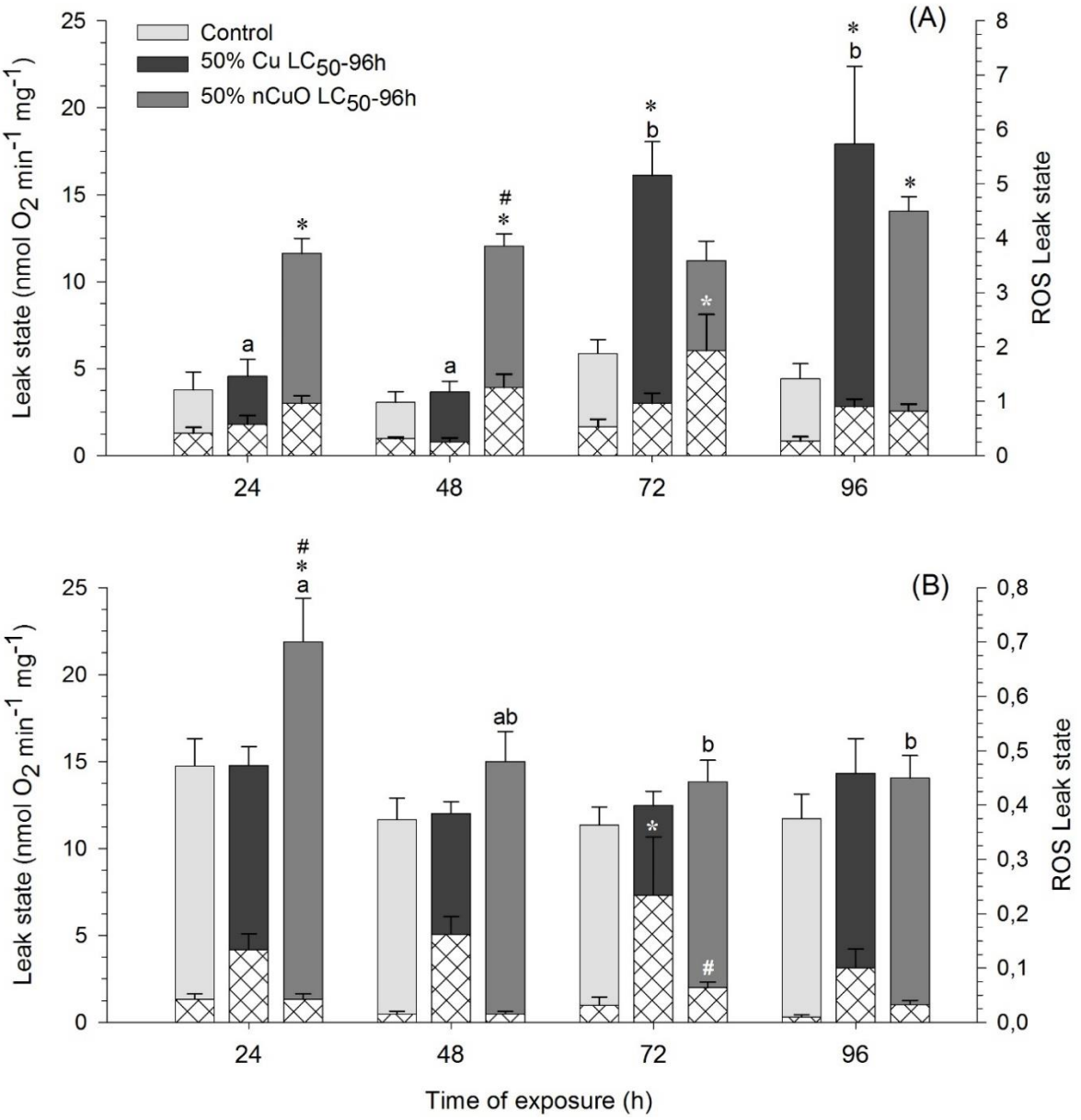

Fig. 6. Mitochondrial Leak state respiration (solid bars) and ROS formation by mitochondrial respiration in Leak state (cross-hatched bars) in gills of (A) *Apistogramma agassizii* and (B) *Paracheirodon axelrodi* after 24, 48, 72 and 96h exposure to 50% of copper LC_{50}-96h and 50% of nanoparticle CuO LC_{50}-96h. Data are presented as Mean±SEM (n=7, at each treatment). Asterisks (*) represents significant differences between the group exposed to either copper or nanoparticle CuO and the control group at each time of exposure ($p<0.05$). Different letters represent statistical differences between the time of exposure within each treatment. (#) represents significant differences between group exposed to copper and nanoparticle CuO at the same time of exposure ($p<0.05$). Note that the scale of ROS production in Leak state of *P. axelrodi* (B) is ten times lower (one order of magnitude) than in *A. agassizii* (A).

Figure 7.

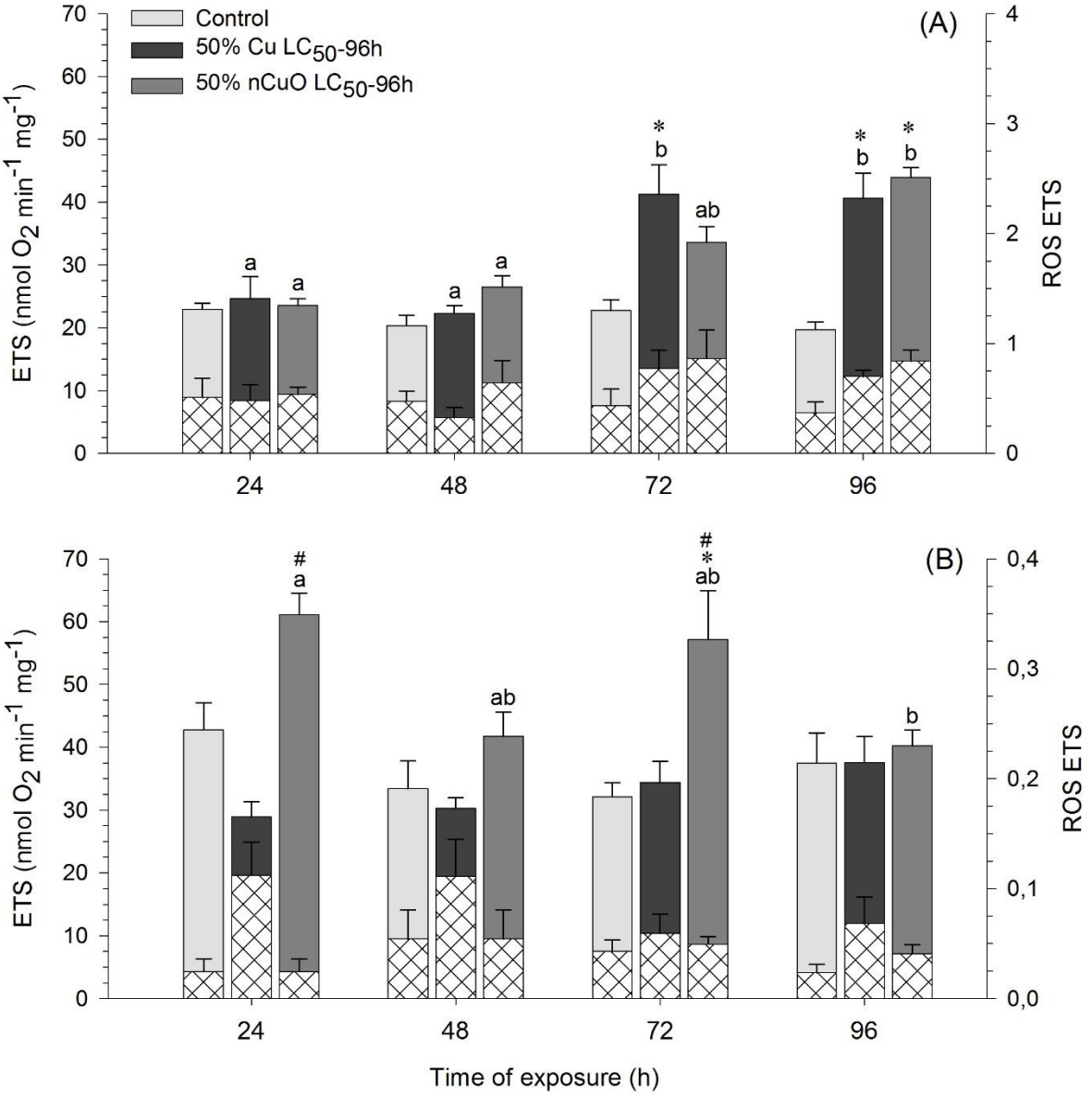

Fig. 7. Mitochondrial ETS (Electron Transport System) respiration (solid bars) and ROS formation by mitochondrial respiration in ETS (cross-hatched bars) in gills of (A) *Apistogramma agassizii* and (B) *Paracheirodon axelrodi* after 24, 48, 72 and 96h exposure to 50% of copper LC_{50}-96h and 50% of nanoparticle CuO LC_{50}-96h. Data are presented as Mean±SEM (n=7, at each treatment). Asterisks (*) represents significant differences between the group exposed to either copper or nanoparticle CuO and the control group, at each time of exposure ($p<0.05$). Different letters represent statistical differences between the time of exposure within each treatment ($p<0.05$). (#) represents significant differences between group exposed to copper and nanoparticle CuO, at the same time of exposure ($p<0.05$). Note that the scale of ROS production in Leak state of *P. axelrodi* (B) is ten times (an order of magnitude) lower than in *A. agassizii* (A).

Figure 8.

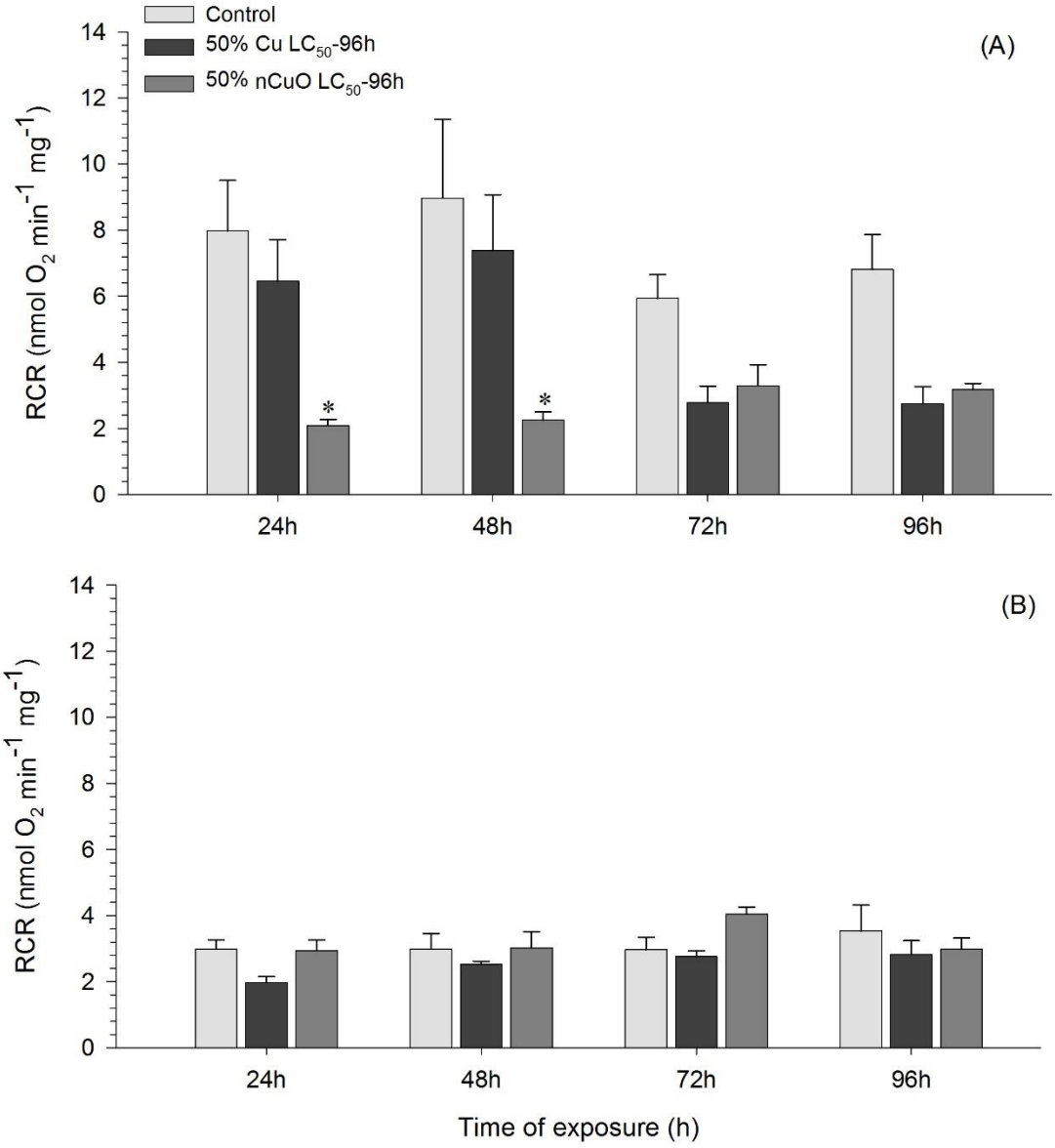

Fig. 8. Mitochondrial Respiratory Control Ratio (RCR) determined as ETS.Leak^{-1} respiration in gills of (A) *Apistogramma agassizii* and (B) *Paracheirodon axelrodi* after 24, 48, 72 and 96h exposure to 50% of copper LC_{50}-96h and 50% of nanoparticle CuO LC_{50}-96h. Data are presented as Mean±SEM (n=7, at each treatment). Asterisks (*) represents significant differences between the group exposed to either copper or nanoparticle CuO and the control group at each time of exposure ($p<0.05$). Different letters represent statistical differences between the time of exposure within each treatment. (#) represents significant differences between group exposed to copper and nanoparticle CuO at the same time of exposure ($p<0.05$).

Table 4. Histopathology and Indexes of Tissue Damage in gills of *Apistogramma agassizii* and *Paracheirodon axelrodi* after 96h of exposure to 50% Cu LC_{50}-96h and 50% nCuO LC_{50}-96h. Values indicate the stages of damage as modified by Poleksic and Mitrovic-Tutundzic (1994). Data are means ± SEM, n = 6.

		A. agassizii			*P. axelrodi*		
	Stage	Control	50% Cu LC_{50}-96h	50% CuO LC_{50}-96h	Control	50% Cu LC_{50}-96h	50% CuO LC_{50}-96h
Filament hyperplasia and hypertrophy	I	0+	0+	+	0+	+	+++
Lamellar hyperplasia and hypertrophy	I	0+	++	+	0+	+++	+++
Lamellar fusion	I	0	0+	+	0	++	0
Lamellar congestion	I	0	0+	0	0	0	0
Lamellar epithelium lifting	I	0	+++	+++	0	+++	+++
Mitochondria rich cells proliferation	I	0	0	+	0	+++	+++
Mucous cells proliferation	I	0	0+	+	0	+++	+++
Edema	I	0	0	0+	0	0	0
Lamellar loss	II	0	0+	0+	0	0+	0
Filament epithelium lifting	II	0	0+	0	0	0	0
Aneurism and rupture	II	0+	++	0+	0+	+	+
Necrosis	III	0	0	0	0	0	0
Fibrosis	III	0	0	0	0	0	
Average histopathological index		**1.4**	**7.4**	**12.8**	**1.4**	**13.0**	**5.6**
Effects		Normal gill function	Normal gill function	Moderate to heavy damage	Normal gill function	Moderate to heavy damage	Normal gill function

Figure 9.

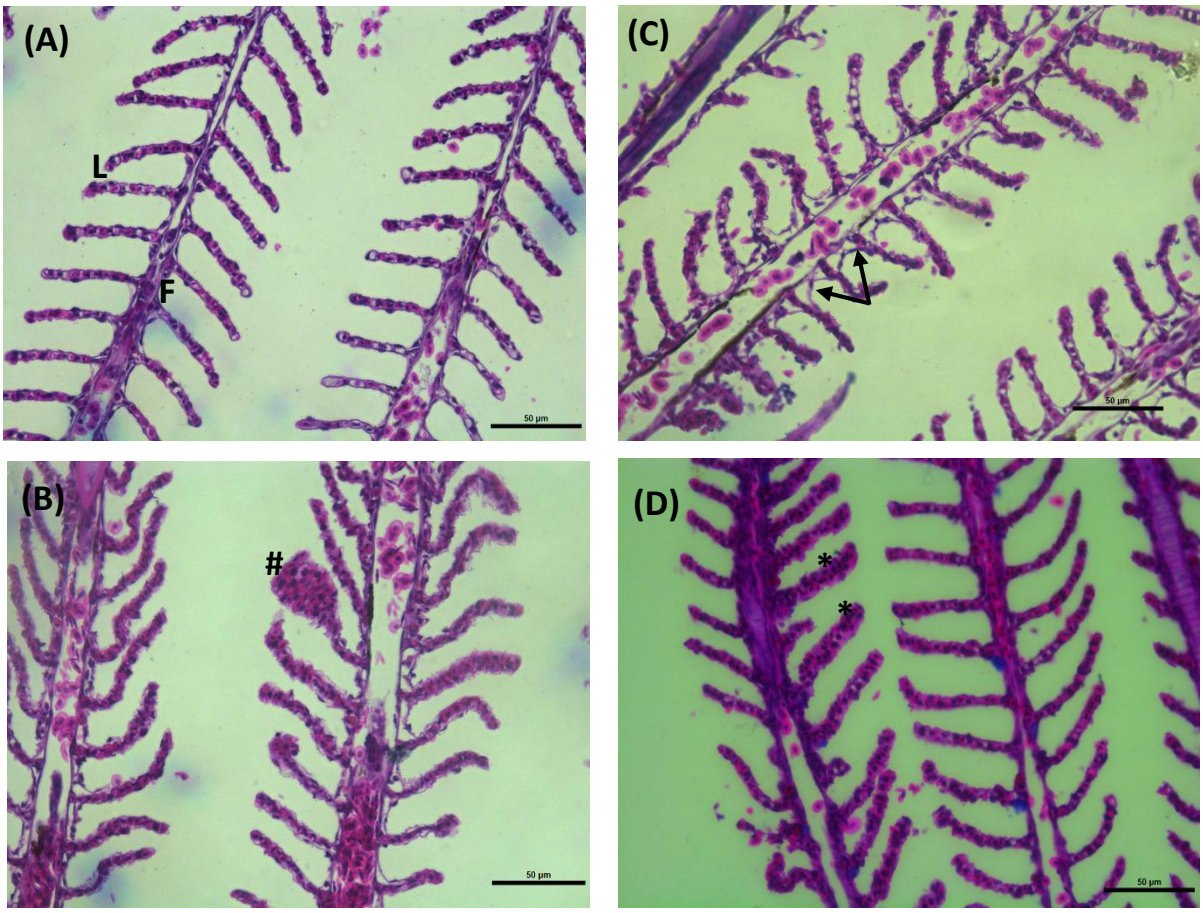

Fig. 9. Representative sections of gill of *Apistogramma agassizii* after 96h exposure to 50% of copper LC_{50}-96h (D) and 50% of nanoparticle CuO LC_{50}-96h (B and C), n=6. (A) control conditions; (B) fillament (#) and hyperplasia and hypertrophy of the fillament epithelium (*); (C) fillament epithelium lifting (←); (D) and hyperplasia and hypertrophy of the fillament epithelium (*). Note the normal structure of the fillament (F) and lamellae (L) in the control. Scale bar = 50 µm for all pictures.

Figure 10.

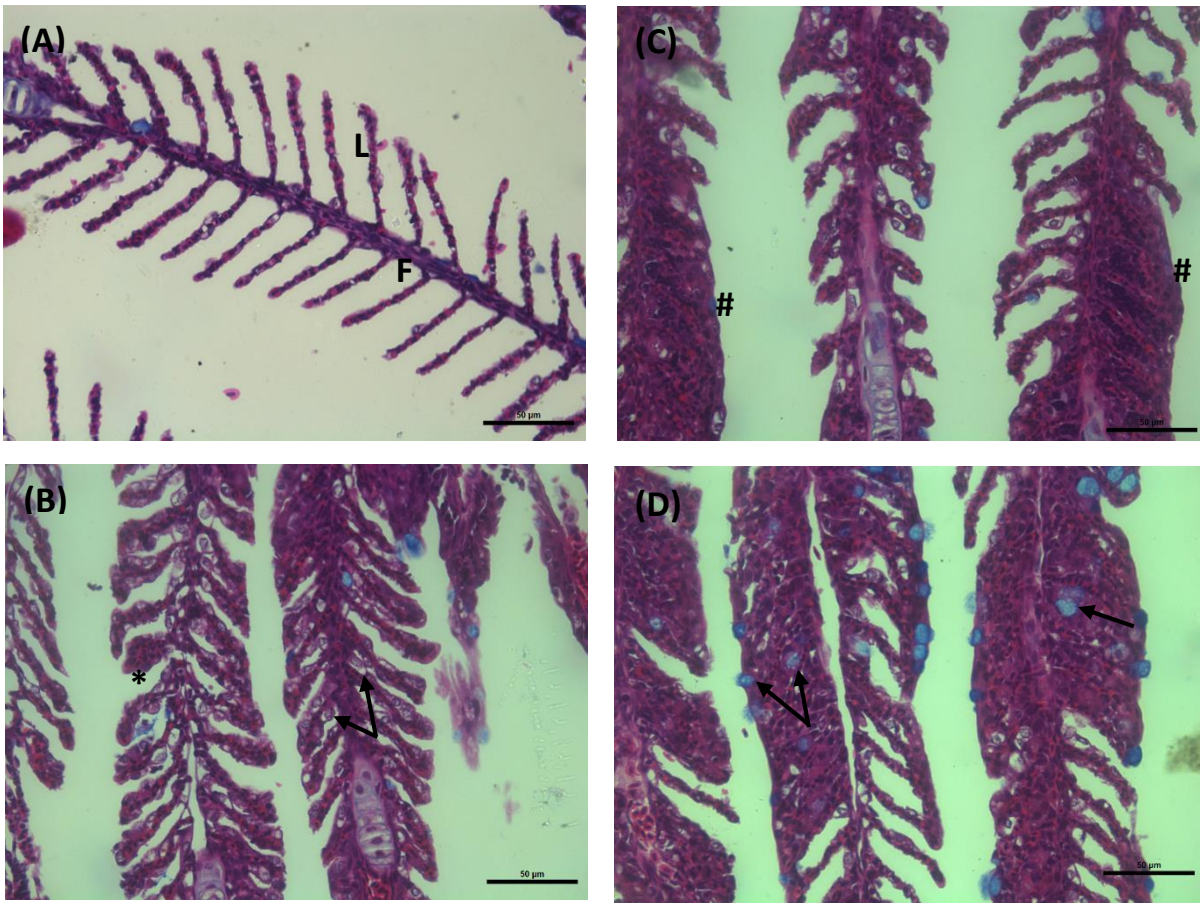

Fig. 10. Representative sections of gill of *Paracheirodon axelrodi* after 96h exposure to 50% of copper LC_{50}-96h (B and D) and 50% of nanoparticle CuO LC_{50}-96h (C), n=6. (A) control conditions; (B) proliferation of mitochondria rich cells (←) and hyperplasia and hypertrophy of the filament epithelium (*); (C) and filament fusion (#); (D) Mucous cells proliferation (←). Note the normal structure of the filament (F) and lamellae (L) in the control. Scale bar = 50 μm for all pictures.

Figura 11.

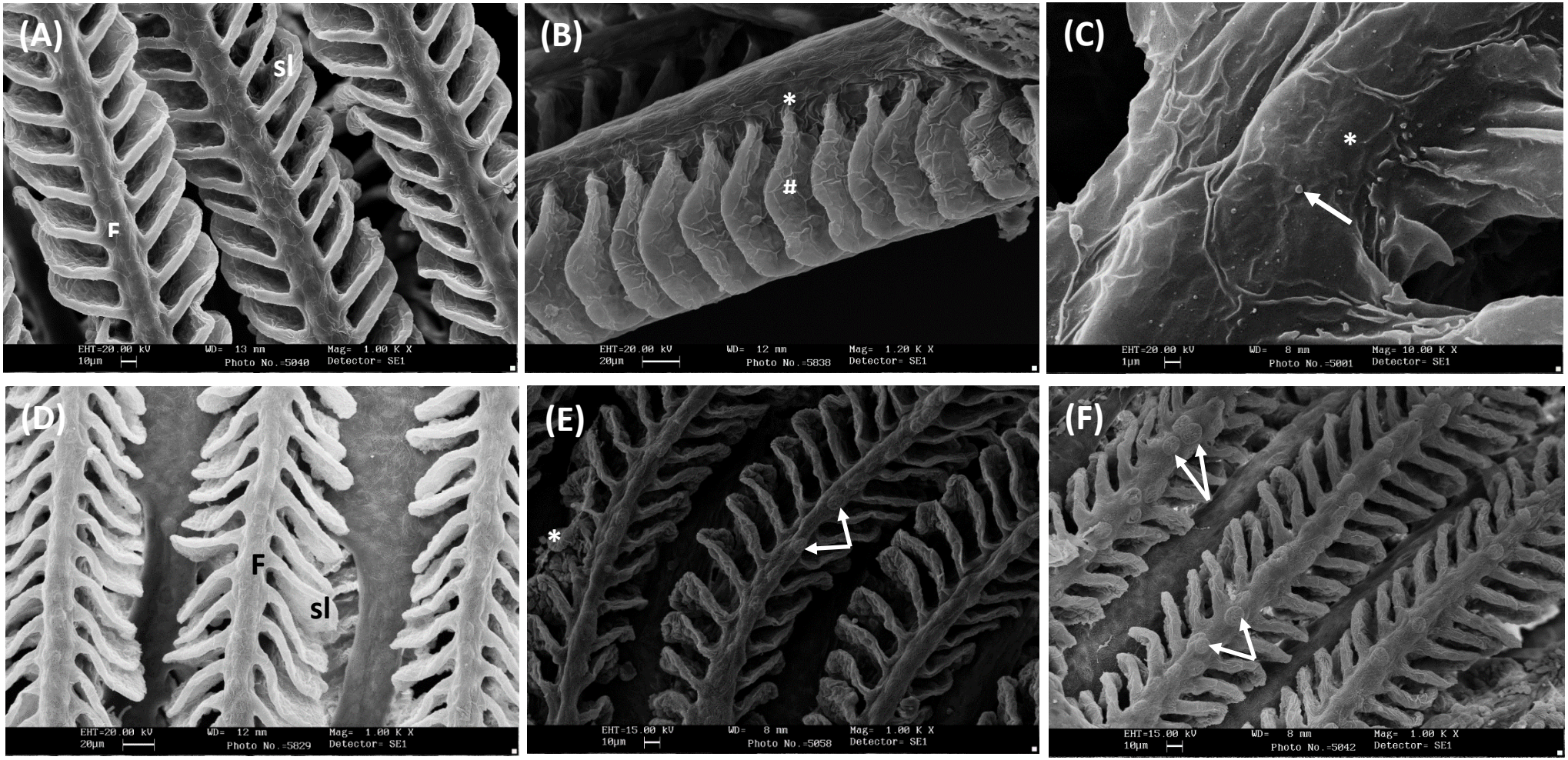

Fig. 11. Scanning electron micrographs of gills filaments of *Apistogramma agassizii* (A: control, B: copper and C: CuO nanoparticle) and *Paracheirodon xelrodi* (D: control, E: copper and F: CuO nanoparticle) after 96h exposure to 50% of copper LC_{50}-96h and 50% of nCuO LC_{50}-96h, n=3. (A and D) regular spacing of secondary lamellae, sl, on the gill fillament, F, (B) epithelium with loss of microridges (*) and lamellar hyperplasia and hypertrophy (#); (C) epithelium with loss of microridges (*) and nanoparticles adhered (arrow). (E) lamellar fusion (*) and gills projections evidentiated (arrow); (F) gills projections strongly evidentiated in nCuO exposure.

Figure 12.

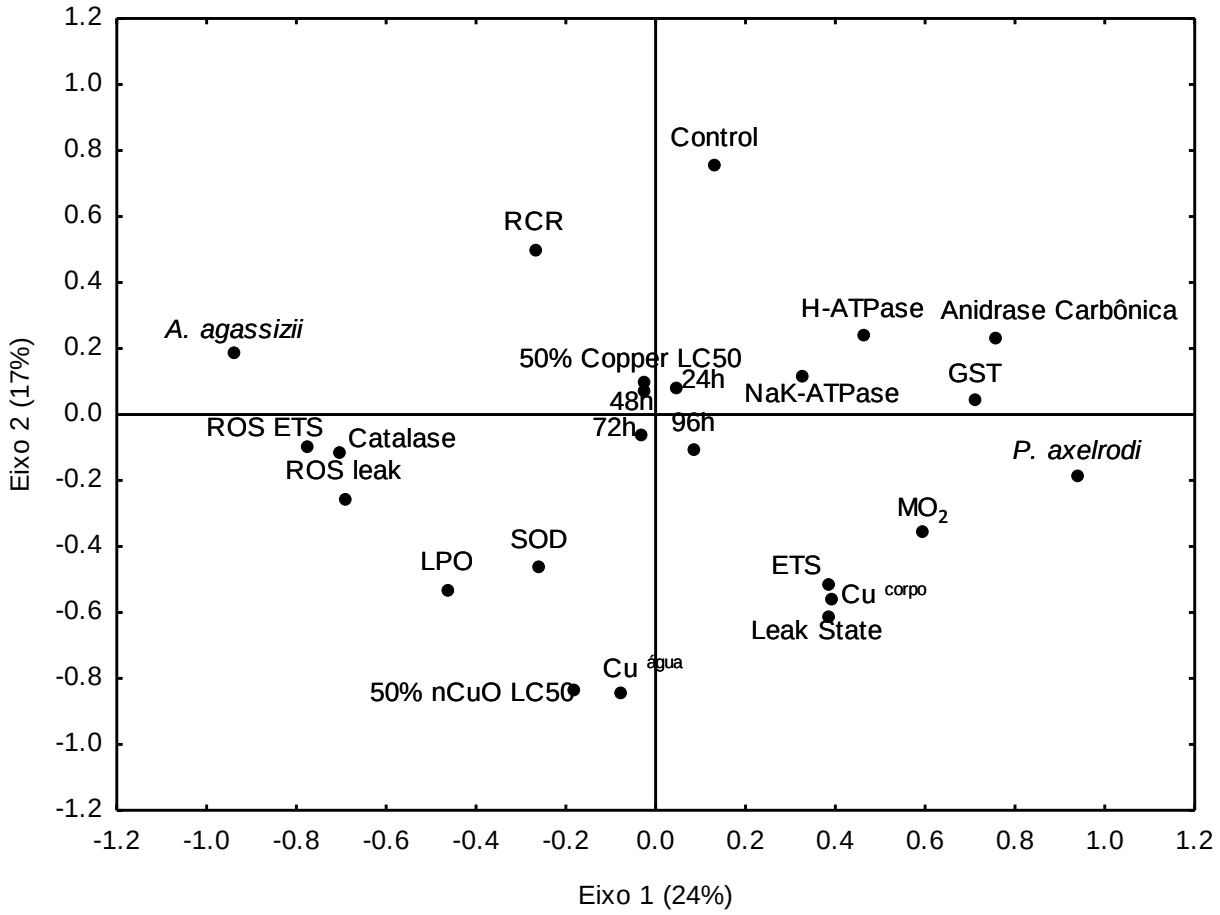

Fig. 12. Principal component analysis of all the parameters analyzed for *A. agassizii* and *P. axelrodi*.

CONCLUSÃO FINAL

O presente trabalho mostrou diferentes sensibilidades das espécies aqui estudadas. Uma idéia geral das disfunções encontradas em cada uma das espécies foi evidenciada nas análises de PCA (Fig. 12), onde as espécies são agrupadas em diferentes extremos, indicando diferentes respostas das funções fisiológicas. Em geral, *A. agassizii* apresentou mais alterações associadas ao estresse oxidativo, que podem ser observadas pelas alterações no sistema antioxidante (atividade de catalase e SOD e níveis de LPO), além da produção ROS tanto no ETS e quanto no Leak state, além desses efeitos serem muito intensificados as exposições à nCuO. Em constraste, *P. axelrodi* mostrou mais efeitos metabólicos, como alterações na MO_2 e disfunções mitocondriais (ETS e H^+ Leak).

Considerando os dados aqui apresentados, sugerimos que *A. agassizii* apresenta um mecanismo de adaptação mitocondrial, uma vez que esta espécie pode desacoplar suas mitocôndrias como resposta ao *feedback* entre a geração de ROS e o extravasamento de prótons na membrana mitocondrial, onde o H^+ leak pode inibir a geração de ROS, ao passo que o ROS estimula o H^+ leak. Assim, como consequencia do aumento dos níveis de ROS após a exposição a nCuO em *A. agassizii*, houve aumento no extravasameto de prótons na matriz mitocondrial, indicando um mecanismo de adaptação deste Cichlidae. A consequencia deste ROS gerado, é a ativação dos mecanismos de defesas oxidants, que podem ter contribuído para a redução dos efeitos histopatológicos nas brânquias desta espécie. Além disso, grande parte dos efeitos em *A. agassizii* foram dependentes do tempo nas exposições à nCuO. Estes resultados podem ser explicados por esta espécie apresentar uma baixa capacidade de transporte e permeabilidade branquial à íons, influenciando diretamente no consumo de oxigênio e na capacidade de absorção e metabolização dos compostos de Cu^{+2}. Por outro lado, *P. axelrodi* mostrou mais disfunções energéticas e osmóticas no cobre dissolvido, e a extensão desse comprometimento não foi dependente do tempo de exposição, indicando um desbalanço no compromisso osmorregulatório. Este Characidae demonstrou um aumento de demandas energéticas, como observado pelo aumento do consumo de oxigênio, que pode ser explicado pelo intenso comprometimento da morfologia das brânquias. *P. axelrodi*, por pertencer à família Characidae, apresenta um sistema de transporte branquial de Na^+ caracterizado por altas taxas de influxo e effluxo desse íon (i.e. maior taxa de *turnover* de Na^+), o que, segundo Grosell et al. (2002), resultaria em reduções mais rápidas do *pool*

interno de Na^+ dos animais durante a exposição ao cobre, o que explicaria a sua maior sensibilidade. Assim, as respostas ionoregulatórias dessa espécie durante a exposição aguda ao cobre levariam a um maior maior gasto energético dos animais para a manutenção do seu balanço iônicoo que, por sua vez, explicaria o aumento do MO_2, e consequente alterações nas funções metabólicas, observados nessa espécies nesse estudo. Nossos resultados revelam diferentes mecanismos de ação tóxica de contaminantes estão associados com diferenças de sensibilidade entre os grupos estudados aqui.

REFERÊNCIAS BIBLIOGRÁFICAS

Almeida, E.; Diamantino, T. C.; Sousa, O. Marine paints: The particular case of antifouling paints. *Prog. Org. Coat.* **2007**, 59, 2-20.

Alsop, D.; Wood, C. M. Metal uptake and acute toxicity in zebrafish: Common mechanisms across multiple metals. *Aquat. Toxicol.* **2011**, 105, 385–393.

Asada, K. Ascorbate peroxidase-a hydrogen peroxide scavenging enzyme in plants. *Physiol. Plant.* **1992**, 67, 235-241.

Bernet, D.; Schmidt, H.; Meier, W.; Burkhardt-Holm, P.; Wahli, T. Histopathology in fish: proposal for a protocol to assess aquatic pollution. *J. Fish. Dis*. **1999**, 22, 25-34.

Beaumont, M. W.; Butler, P. J.; Taylor, E. W. Exposure of brown trout to a sublethal concentration of copper in soft acidic water: effects upon gas exchange and ammonia accumulation. *J. Exp. Biol.* **2003**. 206, 153–162.

Beutler E. 1975. *Red Cell Metabolism: A manual of biochemical methods*. Grune & Straton, New York.

Boveris, A.; Chance, B. The mitochondrial generation of hydrogen peroxide. General properties and effect of hyperbaric oxygen. *Biochem. J*. **1973**, 134, 707-716. DOI: 10.1042/bj1340707.

Bradford, M. M. A rapid and sensitive method for the quantification of microgram quantities of protein utilizing the protein-dye binding. *Analytical Biochemistry*. **1976**, 72, 248-254.

Brand, M. D. Uncoupling to survive? The role of mitochondrial inefficiency in ageing. *Exp Gerontol*. **2000**, 35, 811–820

Brookes, P. S. Mitochondrial H^+ leak and ROS generation: An odd couple. *Free Radical Biol. Med*. **2005**, 38, 12– 23.

Callaghan, N. I.; Allen, G. J. P.; Robart, T. E.; Dieni, C. A.; MacCormack, T. J. Zinc oxide nanoparticles trigger cardiorespiratory stress and reduce aerobic scope in the white sucker, *Catostomus commersonii*. *NanoImpact.* **2016**, 2, 29–37.

Campbell, H. A.; Handy, R. D.; Sims, D. W. Increased metabolic cost of swimming and consequent alterations to circadian activity in rainbow trout (*Oncorhynchus mykiss*) exposed to dietary copper. *Can. J. Fish. Sci.* **2002**, 59, 768-777. DOI: 10.1139/F02-046

Campos, D. F.; Jesus, T. F.; Kochhann, D.; Heinrichs-Caldas, W.; Coelho, M. M.; Almeida-Val, F.M.F. Metabolic rate and thermal tolerance in two congeneric Amazon fishes: *Paracheirodon axelrodi* Schultz, 1956 and *Paracheirodon simulans* Géry, 1963 (Characidae). *Hydrobiologia*. **2017**, 789, 133–142.

Chatterjee, A. K.; Sarkar, R. K.; Chattopadhyay, A. P.; Aich, P.; Chakraborty, R.; Basu, T. A simple robust method for synthesis of metallic copper nanoparticles of high antibacterial potency against *E. coli*. *Nanotechnology*. **2012**, 23, 85–103.

Cheon, J.; Lee, J.; Kim, J. Inkjet printing using copper nanoparticles synthesized by electrolysis. *Thin Solid Films*. **2012**, 520, 2639–2643.

Chowdhury, M. J.; Girgis, M.; Wood, C. M. Revisiting the mechanisms of copper toxicity to rainbow trout: time course, influence of calcium, unidirectional Na^+ fluxes, and branchial Na^+, K^+ ATPase and V-type H^+ ATPase activities. *Aqua Toxicol.* **2016**, 177, 51–62.

Couture, P.; Kumar, P. R. Impairment of metabolic capacities in copper and cadmium contaminated wild yellow perch (*Perca flavescens*). *Aquat. Toxicol*. **2003**, 64, 107-120.

Crémazy, A.; Wood, C. M.; Smith, D. S.; Ferreira, M.S.; Johannsson O. E.; Giacomin, M.; Val, A. L. Investigating copper toxicity in the tropical fish cardinal tetra (*Paracheirodon axelrodi*) in natural Amazonian waters: measurements, modeling, and reality. *Aquat. Toxicol.* **2016**, 180, 353–363.

De Boeck, G.; De Smet, H.; Blust, R. The effect of sublethal levels of copper on oxygen consumption and ammonia excretion in the common carp, *Cyprinus carpio*. *Aquat. Toxicol.* **1995**, 32, 127-141.

De Boeck, G.; Vlaeminck, A.; Blust, R. Effects of sublethal copper exposure on copper accumulation, food consumption, growth, energy storages and nucleic acid content in common carp. *Arch. Environ. Contam. Toxicol*. **1997**, 33, 415-422.

De Boeck, G.; van der Ven, K.; Hattink, J.; Blust, R. Swimming performance and energy metabolism of rainbow trout, common carp and gibel carp respond differently to sublethal copper exposure. *Aquat. Toxicol.* **2006**, 80, 92–100.

De-Jong, W. H.; Borm, P. J. Drug delivery and nanoparticles: Applications and hazards. *Int. J. Nanomedicine*. **2008**, 3, 133-149.

Duarte, R. M.; Menezes, A. C. L.; Rodrigues, L. S.; Almeida-Val, V. M. F.; Val, A. L. Copper sensitivity of wild ornamental fish of the Amazon. *Ecotoxicol. Environ. Saf*. **2009**, 72, 693–698.

Duarte R. M.; Ferreira M. S.; Wood, C. M.; Val, A. L. Effect of low pH exposure on Na^+ regulation in two cichlid fish species of the Amazon. *Comp. Biochem. Physiol. A: Physiol*. **2013**, 166, 441–448.

EPA Science Policy Council- Nanotechnology Workgroup. 2007. U.S. U.S. Environmental Protection Agency Nanotechnology White Paper, February, U.S Environmental protectin Agency.

Giammar, D. E.; Maus, C. J.; Xie, L. Y. Effects of particle size and crystalline phase on lead adsorption to titanium dioxide nanoparticles. *Environ. Eng. Sci.* **2007**, 24, 85–95.

Gnaiger, E.; Kuznetsov, A. V.; Schneeberger, S.; Seiler, R.; Brandacher, G.; Steurer, W.; Margreiter, R. Mitochondria in the cold. In: Life in the Cold (Heldmaier G, Klingenspor M, eds) Springer, Heidelberg, Berlin, New York: 431-42. 2000.

Gonzalez, R. J.; Dalton, V. M.; Patrick, M. L. Ion regulation in ion-poor, acidic water by the blackskirt tetra (*Gymnocorymbus ternetzi*), a fish native to the Amazon River. *Physiol Zool.* **1997**, 70, 428–435.

Gonzalez, R. J.; Preest, M. R. Ionoregulatory specializations for exceptional tolerance of ion-poor, acidic waters in the neon tetra (*Paracheirodon innesi*). *Physiol. Biochem. Zool*. **1999**, 72, 156-163.

Gonzalez, R. J.; Wilson, R. W. Patterns of ion regulation in acidophilic fish native to the ion-poor, acidic Rio Negro. *J. Fish Biol*. **2001**, 58, 1680–1690.

Gonzalez, R. J.; Wilson, R. W.; Wood, C. M.; Patrick, M. L.; Val, A. L. Diverse Strategies for Ion Regulation in Fish Collected from the Ion-Poor, Acidic Rio Negro. *Physiol. Biochem. Zool*. **2002**, 75, 37–47.

Griffitt, R. J.; Weil, R.; Hyndman, K. A.; Denslow, N. D.; Powers, K.; Taylor, D.; Barber, D. S. Exposure to copper nanoparticles causes gill injury and acute lethality in zebrafish (*Danio rerio*). *Environ. Sci. Technol.* **2007**, 41, 8178–8186.

Griffitt, R. J.; Luo, J.; Gao, J.; Bonzongo, J. C.; Barber, D. S. Effects of particle composition and species on toxicity of metallic nanomaterials in aquatic organisms. *Environ. Toxicol. Chem.* **2008**, 27, 1972-1978.

Griffitt, R. J.; Hyndman, K.; Denslow, N. D.; Barber, D. S. Comparison to molecular and histological changes in zebrafish gills exposed to metallic nanoparticles. *Toxicol. Sci*. **2009**, 107, 404–415. doi:10.1093/toxsci/kfn256

Grosell, M.; Nielsen, C.; Bianchini, A. Sodium turnover rate determines sensitivity to acute copper and silver exposure in freshwater animals. *Comp. Biochem. Physiol. C*. **2002**, 133, 287–303.

Grosell, M., Copper. In: Farrell, A. P.; Wood, C. M.; Brauner, C. J. (Eds.), Homeostasis and Toxicology of Essential Metals, Fish Physiology. Academic Press, San Diego, **2012**, 31A, 54–110.

Guo, D.; Bi, H.; Liu B.; Wu, Q.; Wang, D.; Cui, Y. Reactive oxygen species induced cytotoxic effects of zinc oxide nanoparticles in rat retinal ganglion cells. *Toxicol. In Vitro*. **2013**, 27, 731–738.

Handy, R. D.; Von der Kammer, F.; Lead, J. R.; Hassellöv, M.; Owen, R.; Crane, M. The ecotoxicology and chemistry of manufactured nanoparticles. *Ecotoxicology*. **2008**, 17, 287-314. DOI 10.1007/s10646-008-0199-8

Henry, R. P. Techniques for measuring Carbonic Anhydrase activity in vitro. *The Carbonic Anhydrases*. **1991, Chapter 8,** 119-125.

Hristovski, K.; Baumgardner, A.; Westerhoff, P. Selecting metal oxide nanomaterials for arsenic removal in fixed bed columns: from nanopowders to aggregated nanoparticle media. *J. Hazard. Mater*. **2007**, 147, 265–274.

Isani, G.; Falcioni, M. L.; Barucca, G.; Sekar, D.; Andreani, G.; Carpenè E.; Falcioni G. Comparative toxicity of CuO nanoparticles and $CuSO_4$ in rainbow trout. *Ecotoxicol. Environ. Saf.* **2013**, 97, 40–46.

Isaza, F. J.; Castaño, J. G.; Echeverría, F. E. Field study of experimental antifouling paint formulations. *Dyna*. **2011**, 170, 135-143.

Ivask, A.; Juganson, K.; Bondarenko, O.; Mortimer, M.; Aruoja, V.; Kasemets, K.; Blinova, I.; Heinlaan, M.; Slaveykova, V.; Kahru, A. Mechanisms of toxic action of Ag, ZnO and CuO nanoparticles to selected ecotoxicological test organisms and mammalian cells *in vitro*: A comparative review. *Nanotoxicology*, **2014**, 8, 57–71.

Jiang, Z. Y.; Woollard, A. C. S.; Wolff, S. P. Lipid hydroperoxide measurement by oxidation of Fe^{2+} in the presence of xylenol orange. Comparison with the TBA assay and an iodometric method. *Lipids*. **1991**, 26, 853–856. doi:10.1007/BF02536169

Karlsson, H. L.; Cronhlm, P.; Gustafsson, J.; Mölle, L. Copper Oxide Nanoparticles Are Highly Toxic: A Comparison between Metal Oxide Nanoparticles and Carbon Nanotubes. *Chem. Res. Toxicol.*, **2008**, 21, 1726–1732.

Keen, J. H.; Habig, W. H.; Jakobi, W. B. Mechanism for the several activities of the glutathione-S-transferases. *J. Biol. Chem*. **1976**, 251, 6183–6188.

Klaine, S. J.; Alvarez, P. J. J.; Batley, G. E.; Fernandes, T. F.; Handy, R. D.; Lyon, D. Y.; Mahendra, S.; Mclaughlin, M. J.; Lead, J. R. Nanomaterials in the environment: behavior, fate, bioavailability, and effects. *Environ. Toxicol. Chem*. **2008**, 27, 1825–51.

Kültz, D., Somero, G. N. (1995). Osmotic and thermal effects on in situ ATPase activity in permeabilized gill epithelical cells of the fih Gillichthys mirabilis. The Journal of Experimental Biology 198, 1883–1894.

Kumai, Y.; Perry, S. F. Mechanisms and regulation of Na^+ uptake by freshwater fish. *Respir Physiol Neurobiol.* **2012**, 184, 249-56.

Laurén, D. J.; McDonald, D. G. Effects of copper on branchial ionoregulation in the rainbow trout, *Salmo gairdneri*, Richardson. *J. Comp. Physiol*. **1985**, 155, 636-644.

Linder, M. C.; Hazegh-Azam, M**.** Copper biochemistry and molecular biology. *Am. J. Clin. Nutr*. **1996**, 63, 797-811.

Longano, D.; Ditaranto, N.; Cioffi, N.; Di Niso, F.; Sibillano, T.; Ancona, A.; Conte, A.; Del Nobile, M. A.; Sabbatini, L.; Torsi, L. Analytical characterization of laser-generated copper nanoparticles for antibacterial composite food packaging. *Anal. Bioanal. Chem.* **2012**, 403, 1179–1186.

Lynch, I.; Dawson, K. A.; Linse, S. Detecting cryptic epitopes created by nanoparticles. *Sci. STKE*. **2006**, 327, 14.

Marshall, W. S. Na^+, Cl^-, Ca^{2+} and Zn^{2+} transport by fish gills: retrospective review and prospective synthesis. *J. Exp. Zool*. **2002**, 293, 264-283.

Matsuo, A. Y. O.; Val, A. L. *Acclimation* to *humic substances* prevents *whole body sodium loss* and *stimulates branchial calcium uptake capacity* in *cardinal tetras Paracheirodon axelrodi* (*Schultz*) *subjected* to *extremely low p*H. *J. Fish Biol.* **2007**, 70, 989–1000.

McCord, J. M.; Fridovich, I.; Superoxide dismutase, an enzymatic function for erythrocuprein. *J. Biol. Chem.* **1969**, 244, 6049–6055.

Midander, K.; Cronholm, P.; Karlsson, H. L.; Elihn, K.; Möller, L.; Leygraf, C.; Wallinder, I. O. Surface Characteristics, Copper Release, and Toxicity of Nano- and Micrometer-Sized Copper and Copper (II) Oxide Particles: A Cross-Disciplinary Study. *Small*. **2009**, 5, 389–399.

Moore, M. N. Do nanoparticles present ecotoxicological risks for the health of the aquatic environment? *Environ. Int.* **2006**, 32, 967–976.

Mueller, N. C.; Nowack, B. Exposure modeling of engineered nanoparticles in the environment. *Environ. Sci Technol.* **2008**, 42, 4447–4453.

Noctor, G.; Arisi, A. C. M.; Jouanin, L.; Kunert, K. J.; Rennenberg, H.; Foyer, C. H. Glutathione: biosynthesis, metabolism and relationship to stress tolerance explored in transformed plants. *J. Exp. Bot.* **1998**, 49, 623–647.

Nowack, B., Bucheli, D.T. Occurrence: behaviour and effects of nanoparticles in the environment. *Environ. Pollut*. **2007**, 150, 5–22.

Perreault, F.; Oukarroum, A.; Pirastru, L.; Sirois, L.; Matias, W. G.; Popovic, R. Evaluation of copper oxide nanoparticles toxicity using chlorophyll a fluorescence imaging in *Lemna gibba*. *J. Bot*. **2010**, 10. DOI:10.1155/2010/76314

Perry, S. F. The chloride cell: Structure and Function in the Gills of Freshwater Fishes. *Annu. Rev. Physiol*. **1997**, 59, 325–47.

Petosa, A. R.; Jaisi, D. P.; Quevedo, I. R.; Elimelech, M.; Tufenkji, N. Aggregation and Deposition of Engineered Nanomaterials in Aquatic Environments: Role of Physicochemical Interactions. *Environ. Sci. Technol*. **2010**, 44, 6532–6549.

Richter, C.; Park, J. W.; Ames, B. N. Normal oxidative damage to mitochondrial and nuclear DNA is extensive. *Proc. Natl. Acad. Sci*. **1988**, 85, 6465–6467.

Poleksic, V.; Mitrovic-Tutundzic, V. Fish gills as a monitor of sublethal and chronic effects of pollution. In: Müller, R. & R. Lloyd (Eds.). Sublethal and Chronic effects of pollutants on freshwater fish. Oxford, Fishing News Books. **1994**, 339-352.

Pörtner, H. O. Climate variations and the physiological basis of temperature dependent biogeography: systemic to molecular hierarchy of thermal tolerance in animals. *Comp. Biochem. Physiol. A: Physiol*. **2002,** 132, 739-761.

Raffi, M.; Mehrwan, S.; Bhatti, T. M.; Akhter, J. I.; Hameed, A.; Yawar, W.; Hasan, M. Investigations into the antibacterial behavior of copper nanoparticles against *Escherichia coli*. *Ann Microbiol*. **2010**, 60, 75–80. DOI 10.1007/s13213-010-0015-6

Roco, M. C. Nanotechnology: convergence with modern biology and medicine. *Curr. Opin. Biotechnol*. **2003**, 14, 337–46.

Rothen-Rutishauser, B. M.; Schürch, S.; Haenni, B.; Kapp, N.; Gehr, P. Interaction of fine particles and nanoparticles with red blood cells visualized with advanced microscope techniques. *Environ. Sci. Technol.* **2006**, 40, 4353–4359. **DOI:** 10.1021/es0522635

Saison, C.; Perreault, F.; Daigle, J. C.; Fortin, C.; Popovic, R. Effect of coreshell copper oxide nanoparticles on cell culture morphology and photosynthesis (photosystem II energy distribution) in the green alga, *Chlamydomonas reinhardtii*. *Aquat. Toxicol.* **2010**, 96, 109–114.

Salin, K.; Auer, S. K.; Rudolf, A. M.; Anderson, G.; Cairns, A. G.; Mullen, W.; Hartley, R. C.; Selman, C.; Metcalfe, N. B. Individuals with higher metabolic rates have lower levels of reactive oxygen species *in vivo*. *Biol. Lett.* **2015**, 11, 20150538. http://dx.doi.org/10.1098/rsbl.2015.0538

Sampaio, A. Q.; 2000. Caracterizac¸ ão física e química dos sedimentos na área do Distrito Industrial de Manaus (AM). Ph.D. Dissertation. Universidade Federal do Amazonas, Manaus, AM Brazil.

Sappal, R.; MacDonaldb, N.; Fast, M.; Stevens, D.; Kibengea, F.; Siahc, A.; Kamunde, C. Interactions of copper and thermal stress on mitochondrial bioenergetics in rainbow trout, *Oncorhynchus mykiss*. *Aquat. Toxicol.* **2014**, 157, 10–20.

Sappal, R.; MacDougaldc, M.; Fast, M.; Stevens, D.; Kibengea, F.; Siahd, A.; Kamunde C. Alterations in mitochondrial electron transport system activity in response to warm acclimation, hypoxia-reoxygenation and copper in rainbow trout, *Oncorhynchus mykiss*. *Aquat. Toxicol*. **2015**, 165, 51–63.

Schindler, P. W.; Stumm, W. The surface chemistry of oxides, hydroxides and oxide minerals. In: *Aquatic Surface Chemistry*; Wiley, S. W., Eds; New York, **1987**, 83–110.

Service, R. F. Nanotoxicology. Nanotechnology grows up. *Science*. **2004**, 304, 1732–1734. DOI:10.1126/science.304.5678.1732

Shaw, B. J.; Al-Bairuty, G.; Handy, R. D. Effects of waterborne copper nanoparticles and copper sulphate on rainbow trout, (*Oncorhynchus mykiss*): Physiology and accumulation. *Aquat. Toxicol*. **2012**, 116–117, 90–101. DOI:10.1016/j.aquatox.2012.02.032

Shaw, B. J.; Handy, R. D. Physiological effects of nanoparticles on fish: A comparison of nanometals versus metal ions. *Environ. Int*. **2011**, 37, 1083–1097.

Siddiqui, S.; Goddard, R. H.; Bielmyer-Fraser, G. K. Comparative effects of dissolved copper and copper oxide nanoparticle exposure to the sea anemone, *Exaiptasia pallida*. *Aquat. Toxicol*. **2015**, 160, 205–213.

Sies, H. Glutathione and its role in cellular functions. *Free Radical Biol. Med.* **1999**, 27, 916–921.

Silva, M. S. R.; Ramos, J. F.; Pinto, A. G. N. Metais de transição nos sedimentos de Igarapés de Manaus-AM. *Acta Limnol. Bras.* **1999**, 11, 89–100.

Smart, S. K.; Cassady, A. I.; Lu, G. Q.; Martin, D. J. The biocompatibility of carbono nanotubes. *Carbon*. **2006**, 44, 1034–1047. doi:10.1016/j.carbon.2005.10.011

Staniek, K.; Nohl, H. H_2O_2 detection from intact mitochondria as a measure for one-electron reduction of dioxygen requires a non-invasive assay system. *Biochim. Biophys. Acta*. **1999**, 1413, 70–80.

Starkov, A. A.; Fiskum, G. Regulation of brain mitochondrial H2O2 production by membrane potencial and NA(P)H redox state. *J. Neurochem*. **2003**, 86, 1101-1107. **DOI:** 10.1046/j.1471-4159.2003.01908.x

Steffensen, J. Some errors in respirometry of aquatic breathers: How to avoid and correct for them. *Fish Physiology* and *Biochemistry*. **1989**, 6, 49-59.

Studer, A. M.; Limbach, L. K.; Van Duc, L.; Krumeich, F.; Athanassiou, E. K.; Gerber, L. C.; Moch, H.; Stark, W. J. Nanoparticle cytotoxicity depends on intracellular solubility: Comparison of stabilized copper metal and degradable copper oxide nanoparticles. *Toxicol. Lett.* **2010**, 197, 169-174.

Tilaki, R. M.; Iraji Zad, A.; Mahadavi, S. M.; Size, composition and optical properties of copper nanoparticles prepared by laser ablation in liquids. *Appl. Phys. A.* **2007**, 88, 415–419.

Turrens, J. F. Superoxide Production by the Mitochondrial Respiratory Chain. *Biosci Rep.* **1997**, 17. DOI: 10.1023/A:1027374931887

Van der Meer, D. L., van den Thillart, G. E., Witte, F., de Bakker, M. A., Besser, J., Richardson, M. K., Spaink, H. P., Leito, J. T. and Bagowski, C. P. (2005). Gene expression profiling of the long-term adaptive response to hypoxia in the gills of adult zebrafish. *Am. J. Physiol.* 289, R1512-R1519.

Verdouw, H.; Van Echteld, C. J. A.; Dekkers, E. M. J. Ammonia determination based on indophenol formation with sodium salicylate. *Water. Res*. **1978**, 12, 399-402.

Vitale, A. M.; Monserrat, J. M.; Castilho, P.; Rodriguez, E. M. Inhibitory effects of cadmium on carbonic anhydrase activity and ionic regulation of the estuarine crab *Chasmagnathus granulata* (Decapoda, Grapsidae). *Comp. Biochem. Phys C* . **1999**, 122, 121–129.

Wood, C. M.; Robertson, L. M.; Johannsson, O. E.; Val, A. L. Mechanisms of Na^+ uptake, ammonia excretion, and their potential linkage in native Rio Negro tetras (*Paracheirodon axelrodi*, *Hemigrammus rhodostomus*, and *Moenkhausia diktyota*). *J Comp Physiol B*. **2014**, 184, 877–890.

Wood, C. M.; Netto, J. G. S.; Wilson, J. M.; Duarte, R. M.; Val, A. L. Nitrogen metabolism in tambaqui (*Colossoma macropomum*), a neotropical model teleost: hypoxia, temperature, exercise, feeding, fasting, and high environmental ammonia. *J Comp Physiol B*. **2017**, 187, 135–151.

Wu, Z.; Yangb, S.; Wu, W. Shape control of inorganic nanoparticles from solution. ***Nanoscale***, **2016**, **8**, 1237-1259.

Xiong, S.; George, S.; Yu, H.; Damoiseaux, R.; France, B.; Ng, K. W.; Loo, J. S. C. Size influences the cytotoxicity of poly (lactic-co-glycolic acid) (PLGA) and titanium dioxide (TiO_2) nanoparticles. *Arch Toxicol*. **2013**, 87, 1075–1086.

Yan, J. J.; Chou, M. Y.; Kaneko, T.; Hwang, P. P. Gene expression of Na^+/H^+ exchanger in zebrafish H^+ -ATPase-rich cells during acclimation to low-Na+ and acidic environments. *Am. J. Physiol. Cell Physiol*. **2007**. 293, C1814-C1823.

Zall, D. M.; Fisher, D.; Garner, M. Q. Photometric determination of chlorides in water. *Anal. Chem.* **1956**, 28, 1665-1678. Doi: 10.1021/ac60119a009.